March 2018

Observing the Molecular Basis of Thin Filament Activation with a Three Bead Laser Trap Assay

Thomas Longyear

Observing the Molecular Basis of Thin Filament Activation with a Three Bead Laser Trap Assay

A Dissertation Presented

by

THOMAS J. LONGYEAR

Submitted to the Graduate School of the University of Massachusetts
In partial fulfillment of the requirements for the degree of

DOCTOR OF PHILOSOPHY

February 2018

Department of Kinesiology

Observing the Molecular Basis of Thin Filament Activation with a Three Bead Laser Trap Assay

A Dissertation Presented

by

THOMAS J. LONGYEAR

Approved as to style and content by:

_____
Edward P. Debold, Chair

_____
Mark S. Miller, Member

_____
Jennifer Ross, Member

_____
Jane Kent, Department Chair
Department of Kinesiology

DEDICATION

To Christine, for her faith and reassurance.

ACKNOWLEDGEMENTS

First and foremost, I'd like to thank my advisor and mentor Dr. Debold for taking a chance on me and accepting me as a graduate student. I'm grateful for many things, but I'm especially grateful for your open door and your open mind. Thank you for all the one-on-one meetings and the encouragement during my time here.

I'm also grateful for the education and support provided by key faculty members. To Jane Kent, for being tough but fair, and believing I could make it this far when I wasn't so sure. To Jenny Ross, for not only be the smartest person I know, but probably the best educator as well. To Mark Miller, for being logical and even-keeled, characteristics that I hold in high regard.

To my peers in the Department of Kinesiology at the University of Massachusetts, I'm thankful for the challenging conversations and debates, the humor, and for being comrades-in-arms through the struggle. To the people that make this department run so well, especially the women in the front office. Thank you for helping in so many ways and so many times when I didn't have my act together.

To my parents, who I can't thank enough for the love and support. Thank you for being such great role models.

Lastly, and most of all, I want to thank Christine, the love of my life. I don't know if I could have done this without you. Thank you so much for being grounded and faithful. Thank you for being my rock.

ABSTRACT

OBSERVING THE MOLECULAR BASIS OF THIN FILAMENT ACTIVATION WITH A THREE BEAD LASER TRAP ASSAY

FEBRUARY 2018

THOMAS J. LONGYEAR, B.S., UNIVERSITY OF ALABAMA HUNTSVILLE

M.S., UNIVERSITY OF MASSACHUSETTS

Ph.D., UNIVERSITY OF MASSACHUSETTS

Directed by: Professor Edward P. Debold

Muscle contracts after calcium (Ca^{++}) is released into the muscle cell, resulting from a cascade of events which result in myosin, the molecular motor of muscle, to produce force and motion. Myosin cyclically binds to a regulated thin filament, using the chemical energy of ATP to produce force and motion. Perturbations in muscle, such as a build-up of metabolic by-products or point mutations in key contractile proteins, can inhibit these functions in both skeletal and cardiac muscle either acutely or chronically. Despite the many years we have studied skeletal and cardiac muscle, we still do not have a clear picture of the effect of these perturbations at the molecular level. Indeed, we do not even have a clear picture of how muscle is activated at the molecular level. Such an understanding would provide a foundation for future work, and aid our understanding of perturbations such as muscle fatigue or point mutations. Recent advances in biophysical techniques have allowed us to directly observe both single myosin and small ensembles of myosin interacting with an actin filament. We build off this previous work by examining 1) a single myosin molecule interacting with a regulated actin thin filament, and 2) small ensembles of myosin working together to pull on a regulated thin filament. We set out to directly determine how Ca^{++} and myosin activate the thin filament and thus

muscle. Our approach to directly observe these molecular phenomena across physiological Ca^{++} levels as well as high ATP concentrations is novel. The first goal of this work was to examine how 1) a single myosin interacts with a regulated thin filament and 2) how a small ensemble of myosins work together to generate force and motion in a Ca^{++} dependent manner as they interact with a regulated thin filament. The findings build on previous work using similar techniques, but are rich in data and provide a more physiological viewpoint. The second goal of this work was to examine a particular mutation that leads to hypertrophic cardiomyopathy. The current evidence suggests that this mutation alters both thin filament dynamics and myosin kinetics. This mutation was thus chosen not only to add to our understanding of this particular mutation in hopes of developing a therapeutic, but also to provide insight into the role of thin filament activation and myosin dynamics in hopes of better understanding muscle contraction overall. With our experiments, supplemented with a mathematical model, we have de-convolved the role of Ca^{++} and myosin in thin filament activation, and developed a model of muscle activation from the single molecule up to the scale of a cell.

TABLE OF CONTENTS

Page

LIST OF TABLES

Table Page

LIST OF FIGURES

CHAPTER 1

INTRODUCTION

For over 100 years, the machinery and mechanism for muscle contraction has been studied. Despite this long history, there are many unresolved questions, particularly on the molecular level. How a single myosin molecule interacts with a regulated actin filament (also called a 'regulated thin filament') is unknown. Further, how a small ensemble of myosins work together to bind to a regulated actin filament to produce force and motion is not clear. Considering *in vivo* muscle is structured so that a small ensemble of myosins interact with a regulated thin filament, experiments that can directly observe these conditions would be extremely valuable. We know that during a muscle contraction, calcium (Ca^{++}) is released into the muscle cell, leading to partial activation of the regulated thin filament. Myosin can then strongly bind to the thin filament, leading to complete activation. However, the details of this thin filament activation are unclear. The relative contribution of Ca^{++} and myosin to thin filament activation is of particular interest if we are to better understand the molecular processes of muscle. The complete understanding of thin filament activation is applicable to many conditions, including submaximal Ca^{++}, muscle fatigue, or point mutations.

Muscle fatigue is defined as a transient decrease in the generation of force and/or velocity in response to exercise (32, 38). Muscle fatigue has fundamental implications for exercise physiology, but is also a debilitating symptom of heart failure, which limits physical activity and negatively impacts the patient's prognosis (43, 99). Despite the importance and history of muscle fatigue, the etiology of fatigue is not fully understood. A major hurdle to our understanding is our inability to observe molecular phenomena that

cause muscle fatigue. In fact, the inability to observe molecular phenomena has hindered our understanding of the molecular machinery of muscle even under normal conditions, let alone fatigue like conditions. Before further examining the etiology of fatigue, a better understand how the molecular machinery of muscle works under normal conditions would be of great benefit. A major goal of this dissertation was to provide insight into the molecular details of muscle contraction, and lay a foundation for future work the examine the molecular details of muscle fatigue.

Macroscale experiments that include human or animal participants, whole muscle, and even single muscle fibers have been informative, but are unable to provide information on the molecular details of muscle function, and thus muscle fatigue. Despite a long history of study, only in the last 20 years have we been able to directly examine muscle structure and function at the single molecule level (37). With new techniques now in hand, such as the laser trap assay, a better understanding of muscle function on the molecular level can be obtained. We can now examine the role of myosin and the regulatory proteins during muscle activation.

What follows is a description of our current understanding of the molecular machinery of muscle, including myosin and the regulated thin filament. In addition, we will discuss how this machinery and its function leads to macroscopic observations, and how these observations change with perturbations such as fatigue or mutations in key contractile proteins. Finally, we will discuss experiments that can be performed that would address our questions about myosin's function and thin filament activation under normal conditions, as well as under conditions with specific perturbations.

At the molecular level, muscle contraction is driven by myosin, which is the molecular motor in muscle. Myosin is an ATPase, converting the chemical energy of ATP into mechanical work. Within a muscle fiber, myosin molecules are organized into a

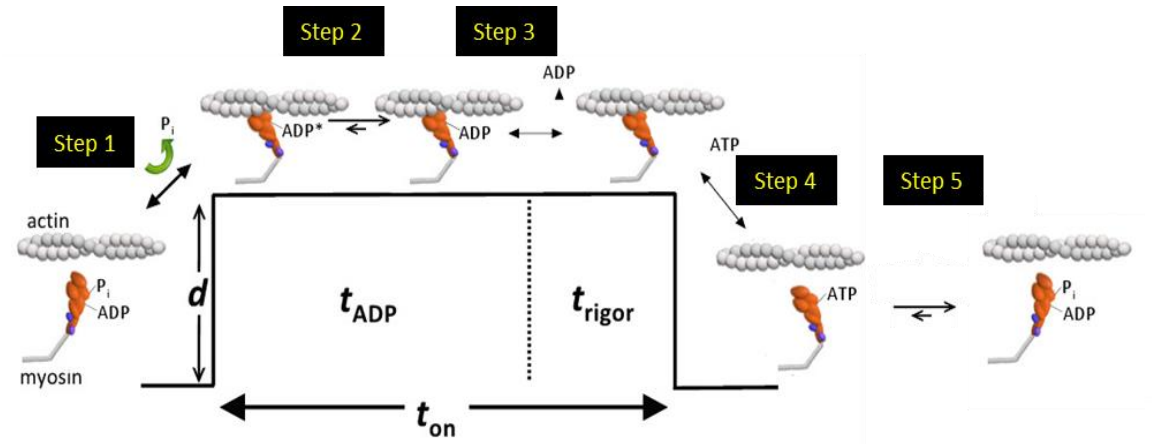

Figure 1.1 Model of the crossbridge cycle. During skeletal muscle contraction, myosin strongly binds to actin, releases Pi, and generates a powerstroke (step 1). Myosin then goes through an isomerization (with no biochemical change, step 2) and then releases ADP (step 3). ATP then binds to myosin, causing actomyosin dissociation (step 4). Myosin then hydrolyzes ATP (step 5) and the cycle repeats. It is possible that acidosis slows each of these steps.

thick filaments and are able to bind to the thin filament, composed of actin. The myosin molecules cyclically bind to the thin filament, producing force and motion with each binding event. This cycle starts when myosin binds to actin and generates a "powerstroke" of approximately 10 nm (figure 1.1, step 1) (25, 37, 119). Myosin then releases one of the ATP hydrolysis products, inorganic phosphate (P_i), into the cytosol, and this release is in close temporal proximity to this powerstroke (5, 20, 33). Some hypothesize that myosin then goes through an isomerization (26, 106), where there is some slight structural change without a biochemical change (step 2) (21, 26, 106). Myosin then releases ADP into the cytosol (step 3) and an ATP molecule will then bind to myosin, causing dissociation of myosin and actin (step 4). Myosin will hydrolyze the ATP (step 5) and the cycle repeats; this cycle is known as the "crossbridge cycle". Each cycle generates an approximate 10 nm displacement. Thus, the faster myosin can move

through the cycle, the more displacement will be generated in a given time, and therefore more velocity is generated. Because myosin is the molecular motor of muscle, the speed at which the crossbridge cycle occurs is the direct cause of muscle contraction velocity. In addition, the force muscle produces is the product of the number of myosin's attached to the regulated thin filament and how much force each myosin produces.

In order to fully understand the crossbridge cycle, we need to know how the myosins interact with regulated actin, as is the case *in vivo*. Our understanding should include not only rested conditions, but also conditions observed during fatigue *in vivo*. These fatigue conditions can alter myosin's function, resulting in changes in thin filament activation. Previous work has shown that specific changes within the muscle that occur during fatigue (13, 23, 64) lead to a reduction in force and velocity, most likely by altering myosin's crossbridge cycle. For example, reducing the pH from 7.0 to 6.2 led to a decrease in force by 3-14%, velocity by 10-30%, and power by 34% (63, 67, 88). However, which step(s) of the crossbridge cycle are affected by acidosis is unclear. ATP hydrolysis, myosin's strong binding to the thin filament, and/or ADP release may be altered; however, this has not been directly observed (25, 82, 100, 105). In addition, there is evidence that acidosis alters myosin's force generating capacity (82). Previous work in single muscle fibers has suggested that a decrease in pH from 7.0 to 6.2 leads to a decrease in stiffness by approximately 25% (82). However, these data were collected with single muscle fibers (which contain billions of myosin molecules) at below physiological temperatures (10 or 15° C). Such experiments with billions of myosin molecules don't provide direct insight into the effects of acidosis on myosin's function, and temperature has been shown to have a significant impact on myosin's on-rate as well

as the effect of acidosis (95, 96, 137). Experiments with a single myosin molecule at near-physiological temperatures (30° C) can be performed with a laser trap assay to address this. This assay can be used to not only understand the molecular details of muscle under normal conditions, but also under fatigue-like conditions. Experiments exploring fatigue can be performed in future work once we have a better picture of how myosin works under normal conditions.

Clearly, myosin plays a key role in muscle's function, and specific perturbations that alter muscle output are due to direct effects on myosin. Additional key players include the regulatory proteins, troponin (Tn) and tropomyosin (Tm). The interaction between myosin and actin is regulated by Ca^{++} binding to troponin. This Ca^{++} binding will lead to a chain of events, involving structural and dynamic changes in troponin, tropomyosin, myosin and actin, eventually leading to muscle contraction. Troponin consists of three subunits: the Ca^{++} binding subunit, troponin C (TnC), the inhibitory subunit, which is responsible for inhibiting contraction during muscle relaxation, troponin I (TnI), and the tropomyosin binding subunit, troponin T (TnT). Ca^{++} binding to TnC leads to slight structural changes the TnC structure, where a hydrophobic patch is exposed on the N-terminus. The C-terminus of TnI, which plays the crucial role of binding to actin and keeping the regulatory proteins in place during relaxation and preventing actomyosin binding, will relieve itself of this duty by releasing actin and binding to the exposed hydrophobic patch. With only minor forces keeping tropomyosin on actin, tropomyosin is now free to slide over the actin surface, which reveals myosin

binding sites on actin (see figure 1.2).

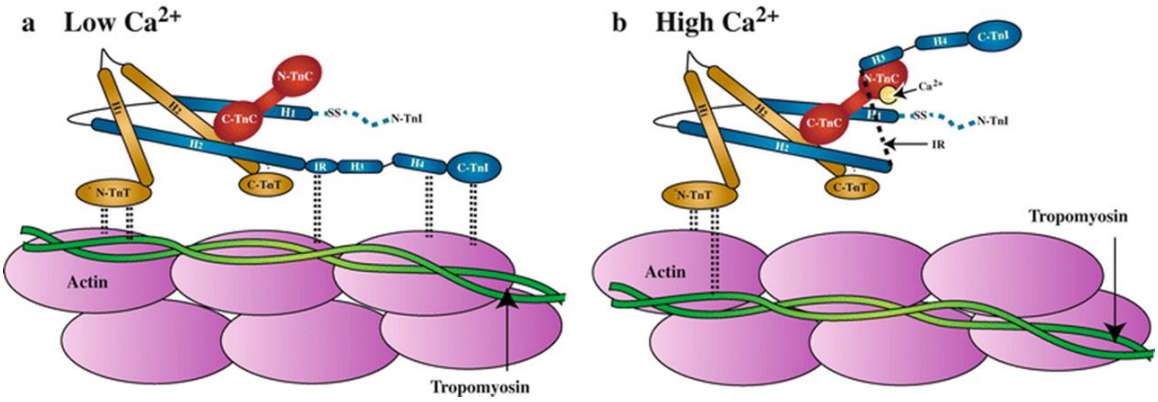

Figure 1.2. Cartoon of TnI at low and high calcium. a) With no calcium bound to troponin C, troponin I stays bound to actin, keeping tropomyosin in the blocked state. b) Upon calcium binding, troponin I detaches from actin and binds to troponin C, allowing tropomyosin to move freely about the actin surface.

The function of regulatory proteins is crucial; minor changes in Ca^{++} concentrations can lead to large changes in troponin and tropomyosin's position on actin, and thus can lead to large changes in muscle force. Therefore, perturbations that alter Ca^{++} binding to troponin or that alter troponin's function can have significant implications. For example, mutations in troponin can lead to cardiomyopathies by presumably altering these Ca^{++}-dependent motions. In addition, during muscle fatigue, Ca^{++} levels decrease (71) and positively charged hydrogen ions may compete with Ca^{++} for binding to troponin (88, 93). Both mechanisms can lead to a drastic reduction in muscle output. The precise molecular mechanisms are unknown.

Prior to Ca^{++} release, tropomyosin is in the "blocked" state, where tropomyosin physically blocks actomyosin binding. Upon Ca^{++} binding to troponin, tropomyosin is moved into the "closed" state, where tropomyosin's position fluctuates across actin's surface and binding sites are transiently available to myosin. Once in the closed state, tropomyosin is pushed into the "open" state upon myosin binding. This premise, known as the three state model, is strongly supported by biochemical experiments (72, 81, 118),

in vitro experiments (29, 62), protein structures (19, 98, 108, 122, 125), and mathematical models (126). Thus, both Ca^{++} binding to troponin and myosin binding to actin are critical to thin filament activation, where thin filament activation is a measure of how available the myosin binding sites on actin are. As stated earlier, perturbations such as troponin mutations or fatigue-like conditions can alter muscle output. In the three-state model, acidosis may block Ca^{++} binding to troponin, potentially keeping tropomyosin in the blocked state. This would result in less actomyosin binding and thus less muscle output. This reduced binding not only affects each myosin, but can also affect neighboring myosin due to the cooperative nature of myosin binding.

A key component of thin filament activation is the cooperative binding of myosin molecules to the regulated thin filament. Once one myosin strongly binds to actin and pushes tropomyosin into the open state, other myosin molecules can more easily bind to actin. Cooperativity can be seen graphically in the pCa-force and pCa-velocity relationships, an example of which is shown in figure 1.3. In this figure, the x-axis is pCa, which represents the negative log of Ca^{++} (pCa 4 is high Ca^{++}, pCa 7 is relatively low Ca^{++}). Force output is very low at low Ca^{++} levels, but as Ca^{++} increases, a drastic increase in force occurs. As more Ca^{++} is present, the regulatory proteins can more readily move out of the blocked state, and myosin can bind. Clearly, both Ca^{++} and

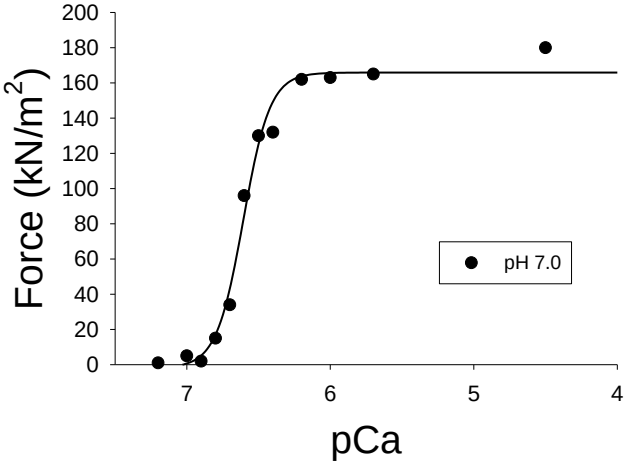

Figure 1.3. Typical force-pCa relationship. A muscle fiber's force generating capacity is dependent on the Ca^{++} concentration. The curve is sigmoidal, and the curve is steep, suggesting high cooperativity.

myosin play a crucial role in thin filament activation, but is one more important than the other? The precise role of each of these players in thin filament activation and cooperativity are not completely understood. Understanding these roles is significant to both skeletal and cardiac muscle because during muscle activation, the physiological Ca^{++} concentration usually lies within the steep portion of the pCa-force relationship. Small changes in Ca^{++} can lead to large changes in myosin binding and subsequent force production. Further, how activation and cooperativity are altered by acidosis and other metabolites produced during fatigue is unclear, though evidence exists that acidosis affects these parameters (22, 24, 88, 93, 133, 135). Therefore, understanding the roles of myosin and Ca^{++} under normal conditions is imperative so that we can better understand the molecular details of fatigue in subsequent experiments. **A key goal of this dissertation was to determine the role of myosin and Ca^{++} in thin filament activation. This was achieved with the state-or-the-art laser trap assay that allows direct observation of single myosin and myosin ensembles generating force. By directly observing the binding of a single myosin or an ensemble of myosin to a regulated thin filament while controlling the level of Ca^{++}, we de-convolved the role of both myosin and Ca^{++} in activation.**

With a better understanding of how myosin and the regulatory proteins lead to thin filament activation, we will be able to understand how specific perturbations affect thin filament activation, as well as cooperativity and the resulting pCa-force relationship. For example, mutant troponins can lead to changes in these measures. The mutations that lead to muscle dysfunction are typically found in key regions of troponin. One key region is the Ca^{++} binding pocket. Obviously, a mutation here could alter Ca^{++} binding and

subsequent thin filament activation. Another key region is the inhibitory region, which binds to actin and prevents tropomyosin from moving and exposing actomyosin binding sites. A mutation in this region could allow tropomyosin to expose actomyosin binding sites in the absence of Ca^{++}. One example of this is a mutation called R146G. This mutation is associated with hypertrophic cardiomyopathy and seems to allow actomyosin binding in the absence of Ca^{++} (34, 70, 114, 129). Unfortunately, the precise mechanism R146G's action is unknown. More precise techniques are required to understand its effect on thin filament activation and potentially help the patients with this mutation. **A second key goal of this dissertation was to examine how R146G has its effects on myosin kinetics and regulated thin filament activation.**

To obtain a better understanding of thin filament activation, experiments on the

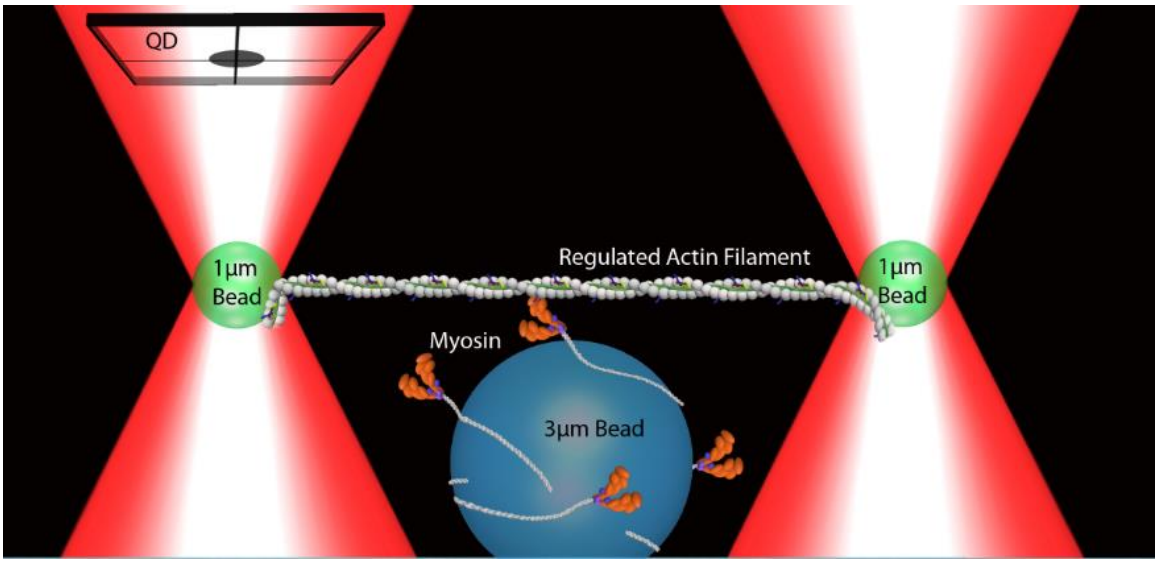

Figure 1.4. Cartoon of the 3-bead assay. Myosin is randomly oriented on the microscope slide surface, occasionally located on a pedestal bead. A bead-filament-bead assembly, trapped by laser light, is put in close vicinity to the pedestal so single molecule interactions can be observed and measured. Figure courtesy of Mike Woodward.

molecular level that can examine a single myosin's ability to interact with the thin filament are crucial. Further, experiments that mimic physiological conditions by examining how a small ensemble of myosin work together to activate the thin filament

could bridge the gap between our current understanding of single myosin molecule kinetics and single muscle fiber experiments. This can be achieved with the 3-bead laser trap assay, where two beads, which are trapped by laser light, hold a single actin filament taught, while a single myosin sitting on a pedestal bead binds to the actin filament (figure 1.4). This technique, with millisecond time and nanometer spatial resolution, allows us to directly observe a single molecule interaction, giving us displacement, duration of attachment, and binding frequency of individual actomyosin interactions. This technique can also be used to examine how multiple myosins pull on a single actin filament cooperatively to generate force.

In addition to collecting novel information on thin filament activation, a key outcome from future work is to be able to use our knowledge of the molecular details to understand how specific perturbations lead to dysfunction. In addition to setting the foundation for examining fatigue, the knowledge gained in this work can set the foundation for examining mutations that cause disease. Our understanding of the molecular details of normal, wildtype proteins can help us construct models for mutations, especially those that cause cardiomyopathies.

The expectation for this dissertation was to create a better understanding of muscle on the molecular level and begin applying that knowledge to specific perturbations. One perturbation that we have gained interest in is the R146G mutation in TnI. This mutation was chosen because it is known to cause cardiomyopathy (60, 65), because of its crucial location in TnI (36, 113, 115), and because the evidence is inconclusive. Though this mutation has been studied previously, there is still little consensus on its effect. For example, some have shown that the R146G negatively affects

force, while others have seen no effect (70, 114, 129, 132). More puzzling is the effect this mutation has on the Ca^{++} dependent production of force and velocity: previous data has shown that force and velocity are reduced at high Ca^{++} compared to wildtype Tn, but force and velocity are increased at low Ca^{++} (12, 60, 69, 70, 114, 129, 132). The molecular mechanisms that lead to these odd phenomena are not well understood. Experiments that examine both thin filament activation as well as myosin kinetics in the presence of this mutation are necessary to gain a full mechanistic understanding of this mutation. By manipulating conditions in an *in vitro* environment, we can gain novel insight into how this mutation causes dysfunction. Future work can then use our understanding of the molecular details of muscle contraction to ameliorate the negative effects of cardiomyopathies.

Overall, the goal of this dissertation was to use state-of-the-art single molecule techniques to better understand regulated thin filament activation. In recent years, many experiments have been performed with either single muscle fibers which contain billions of myosin or with single myosin molecules interacting with an unregulated thin filament. The current dissertation bridges the gap between these two methods by incorporating regulated thin filaments with single, small ensemble, and large ensembles of myosin. This work lays the foundation for future work examining perturbations that cause muscle fatigue. Another key goal was to better understand how a cardiomyopathy mutation in troponin leads to functional changes. These outcomes give us a better understanding of the molecular details of muscle contraction and help us apply our knowledge to attenuate the negative effects of cardiomyopathy mutations.

Hypotheses

Hypothesis 1: Both Ca^{++} and myosin play crucial roles in thin filament activation.

A) During single molecule experiments in the 3-bead assay, myosin's binding to the regulated thin filament will be Ca^{++} dependent.
    a. The frequency of binding will be reduced as Ca^{++} levels are reduced.
    b. The displacement generated upon myosin binding will not be Ca^{++} dependent.

B) During experiments with small ensembles of myosin in the 3-bead assay, the force generated will be Ca^{++} dependent and will show elements of cooperativity.
    a. Many events will be recorded with various forces, and the distributions will shift as Ca^{++} is decreased where force and event frequency will decrease.
    b. The distributions will show cooperativity by containing many events with high force. This cooperative action will be observed by direct observation of moderate forces even at low to moderate calcium (pCa 6-7).
        i. This suggests that once one myosin binds, many others bind as well, leading to a distribution of forces with more high forces than low forces.

C) During experiments with large ensembles of myosin in an *in vitro* motility assay, the velocity generated will be dependent on both ATP, which directly influences the number of myosin bound, and Ca^{++} concentrations.

a. Under conditions of low ATP and low Ca^{++}, velocity will be observed, suggesting that myosin in rigor can activate the thin filament in the absence of Ca^{++}.

b. This suggests that both myosin and Ca^{++} play a role in thin filament activation. Under low ATP and low Ca^{++}, activation is driven by myosins that are strongly bound in a rigor state, while high ATP and high Ca^{++} leads to contributions from both strongly bound myosin and Ca^{++}.

Hypothesis 2: The R146G mutation in troponin I disrupts the normal pCa-velocity relationship by altering multiple steps of the crossbridge cycle.

A) During pCa-velocity experiments, the R146G mutation will lead to enhanced velocity under low Ca^{++} conditions but reduced velocity under high Ca^{++} conditions.

   a. This will lead to a reduced Hill coefficient, which suggests a reduction in cooperativity.

   b. The mutation will also cause an increase in the Ca^{++} sensitivity, as determined by the pCa_{50}.

B) During duty cycle experiments, the R146G mutation will cause an increase in the duty cycle.

   a. This will suggest that the R146G affects myosin kinetics, either increasing the rate of the strong binding step or slowing the rate of ADP release. The most likely steps altered are strong binding and ADP release.

C) During ATP-velocity experiments, the R146 mutation will slow velocity at any given ATP level, suggesting that ADP release is slowed in the presence of the R146G mutation.

CHAPTER 2

LITERATURE REVIEW

The Crossbridge Cycle

Myosin uses energy from ATP hydrolysis to cyclically bind to actin and produce force and motion. This cyclical binding is commonly referred to as the crossbridge cycle. When a muscle is in a resting state, most myosin are in a 'cocked' state, with the myosin head ready to bind to actin and release its hydrolysis products, ADP and P_i. Upon muscle activation, Ca^{++} binds to troponin and the regulatory proteins allow myosin to strongly bind to actin. When this occurs, myosin releases P_i, generates force, and produces an approximate 10 nm displacement of actin, all in a matter of a few milliseconds (37). Myosin continues to produce force as long as it is strongly bound to actin, the duration of which is referred to as "time-on" (t_{on}). During this strongly bound state, there is evidence that myosin isomerizes with ADP still bound (26, 106). Myosin then releases ADP and binds an ATP molecule, which causes dissociation of myosin and actin. From here, myosin can hydrolyze this ATP molecule, which re-cocks the myosin head, and the crossbridge cycle can begin again.

The crossbridge cycle affects force and velocity

To discuss myosin's function, we must discuss what limits myosin's function and its subsequent force and velocity production. The force generated by a muscle fiber is the product of the number of myosin molecules in that fiber strongly bound to actin multiplied by the force per myosin molecule (58, 59). Therefore, the longer myosin stays attached to actin (i.e., t_{on}) relative to the time off of actin (t_{off}), the more myosin molecules will be bound at any given time, increasing the force produced. Based on this,

an increased rate in attachment and a decreased rate of detachment would lead to more myosin bound and thus more force. Experiments performed in the laser trap assay have shown that specific biochemical steps are force dependent, such as ADP release (121). The more force a given myosin is producing, the longer myosin would take to release ADP. This provides a mechanochemical explanation for prolonged attachment and high force production. Velocity, on the other hand, is assumed to be limited by detachment (59, 128), that is, velocity is equal to the displacement generated by myosin divided by the time myosin spends strongly bound to actin (59). The faster myosin can detach, the faster a muscle will contract. This model agrees well with data suggesting that ADP release, an event that occurs with myosin bound to actin, is the biochemical step that limits velocity (91). Simply, force is dependent on myosin being bound to the actin filament, while velocity is dependent on the rate of detachment from the actin filament. This juxtaposition is the basis for the inverse relationship of force and velocity. This relationship was shown in seminal work by A.V. Hill (55) in whole muscle. Evidence that myosin is responsible for this action was demonstrated with the laser trap assay, where a small ensemble of myosin was able to reproduce the force-velocity relationship (27).

Effect of metabolites on the crossbridge cycle

Changes to the concentration of specific metabolites can affect the kinetics of the crossbridge cycle. Some of these metabolites have been suspects for muscle fatigue. This includes ATP, inorganic phosphate (P_i), and acidosis.

ATP

A reduction in ATP was once considered a culprit of fatigue. As ATP concentrations are reduced, the rigor lifetime of a myosin crossbridge increases, which would slow velocity. Current estimates put ATP levels around 5 mM in fresh muscle, and as low as 1 mM in severely fatigued muscle (2). However, 1 mM is more than sufficient. The concentration of ATP that leads to half-maximal binding of myosin, also known as the Km, is approximately 5 uM. Therefore, a decrease to 1 mM would still allow sufficient ATP-myosin binding, and would not have a significant effect on myosin's function.

Inorganic Phosphate (P_i)

Another major culprit of muscle fatigue is inorganic phosphate (P_i). Even small amounts of P_i (5 mM) can negatively impact force (18, 20, 28), though some have postulated that concentrations can reach as high as 30 mM during fatigue (13, 23, 134). P_i release and force generation have been examined extensively, as P_i release is closely associated with force generation and are hard to tease apart. One current hypothesis is that P_i rebinds to actomyosin, inducing dissociation between actin and myosin and thus limiting force production. This hypothesis was validated with single molecule experiments in the laser trap assay recently (28).

Acidosis

Finally, acidosis is likely to be the most studied culprit for muscle fatigue. Acidosis has been proposed to affect more than one step of the crossbridge cycle. Surprisingly, there is relatively little evidence showing which kinetic step is altered. Recent work has shown force to decline 10-18% and velocity to decline by up to 70%

(63, 67, 88). For this to occur, specific steps of the crossbridge cycle must be slowed. Based on the steps that limit force and velocity, three steps are likely slowed: 1) the strong binding, force-generating step, 2) ADP release, and 3) ATP hydrolysis.

The first potential step acidosis may alter is myosin's strong binding to actin. Insightful release and re-stretch experiments performed in single muscle fibers suggested that strong binding was slowed (83). In fact, later work suggested that the acidosis-induced changes observed in both force and velocity could be explained by this one step's rate (105). Additional work comparing the change in force and ATPase as a function of pH also suggested that the rate of attachment is slowed as pH is reduced (100). One technique that could address the rate of strong binding is the single molecule laser trap assay. In this assay, individual binding events between myosin and the thin filament can be directly observed. The rate of strong binding can be determined by recording the number of events over time and determining the binding frequency. This binding frequency can be measured in the presence or absence of acidosis and the effect of acidosis on strong binding can be observed and quantified.

The second kinetic step that could be altered by acidosis is ADP release. There is strong evidence that ADP release is slowed by acidosis, where reducing the pH from 7.4 to 6.4 increased the lifetime of a single actomyosin bond 3-fold (25). This was directly observed in the laser trap assay, where the displacement and binding lifetime of a single myosin molecule interacting with a single filament can be directly observed.

Finally, the third step likely to be altered by acidosis is ATP hydrolysis. The single molecule experiments performed by Debold et al. (25) suggested that ATP hydrolysis was slowed by acidosis. This was suggested based on the average

displacement observed for each powerstroke under various conditions: at low ATP (1 μM), the average displacement was only 2 nm, but this was increased to 6 nm at 10 μM ATP and returned to a normal 10 nm at 1 mM ATP. The authors argue that acidosis does not alter the size of the powerstroke, because the powerstroke size returned to 10 nm at high ATP. Rather, they suggest that ATP hydrolysis is slowed. The logic is as follows: up ATP binding, myosin and actin dissociate (step 4, figure 1). However, if ATP hydrolysis is slowed, myosin may release ATP and bind to actin, forming a strong bond but producing no powerstroke. Thus, in the laser trap assay, an actomyosin binding event would be detected but no displacement generated. If such events happened frequently, the average displacement of all events would be skewed toward values much less than 10 nm, as observed. As ATP concentrations increase to 10 μM and 1 mM, myosin could release ATP, but a new ATP could quickly take its place, and the crossbridge cycle would move forward.

Recent work from our group (26, 76) has teased apart which crossbridge steps acidosis alters. In the presence of acidosis, we observed a slowing of thin filament velocity, which was augmented in the presence of P_i. We postulated that acidosis slows a step during t_{on} (possibly the AM.ADP state), and P_i rebinds to this step, causing dissociation of actomyosin. This agrees well with a detachment-limited model of velocity, where a faster dissociation (caused by P_i) would attenuate acidosis' effect on velocity. We further probed this by measuring velocity in the presence of ADP and P_i. Interestingly, P_i could not attenuate the negative effects of ADP on velocity. We concluded that there are two myosin-ADP states: AM'ADP and AM.ADP, the transition of which is slowed by acidosis. Further, we concluded that P_i can rebind to the AM'ADP

state, causing dissociation and thus limiting acidosis' effects on velocity. However, the addition of ADP leads to an increase in the AM.ADP state, a state that P_i cannot rebind to and thus cannot affect (see Figure 3.1). Further experiments with 2-deoxy-ATP (dATP), an ATP analog, showed that dATP can mitigate the effects of acidosis in the presence or absence of P_i. We concluded that acidosis must slow the weak-to-strong transition, while dATP attenuates this effect. Indeed, previous work has suggested that dATP increases the weak-to-strong transition rate (101, 102).

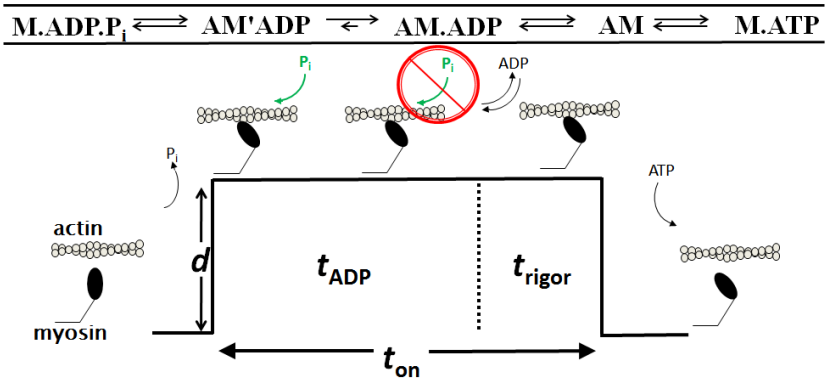

Figure 2.1. Action of Pi rebinding to actomyosin. Pi can rebind to the AM'ADP state, but not the AM.ADP state. Acidosis slows the AM'ADP to AM.ADP transition. Pi can rebind to this state, causing dissociation of actomyosin and thus attenuate acidosis' effect on velocity. The addition of ADP increases the AM.ADP state, a state to which Pi cannot rebind and cannot attenuate velocity.

Though we have made strides toward understanding the effects of acidosis, a clearer picture can be obtained by dissecting each step of the crossbridge cycle. Indeed, single molecule experiments are necessary to directly observe and measure the steps of the crossbridge cycle. One example of the power of single molecule experiments is the results obtained from Debold et al. (25) which directly measured that the rate of ADP release is reduced in the presence of acidosis, in disagreement with inferences made from single fiber data. Additional experiments that could be done to make the conditions more physiological would be to measure the rate of certain kinetic steps in the presence of regulatory proteins. Finally, if ATP hydrolysis is slowed in the presence of acidosis is hard to determine. Debold et al. suggests this is possible, and solution kinetics suggest

that myosin can release ATP and rebind to actin (107). If any step in the crossbridge is slowed by acidosis, myosin's overall rate of ATP hydrolysis, measured as the ATP consumed per second, should decline as the pH is reduced. Interestingly, ATPase experiments have been inconclusive, as some actually suggest an increase in ATPase rate as pH decreases (100), some show no change (7, 8) while others suggest a 10% decrease (109). Clearly, experiments that can tease apart the individual steps of the crossbridge are necessary to characterize acidosis' full effects.

Acidosis may not only affect myosin's kinetic steps, but also the force each myosin can produce. This possibility has been hypothesized previously based on single muscle fiber experiments (82, 100, 105). Some of the evidence is based on assumptions of myosin kinetics based on single fiber measurements (100, 105), while Metzger and Moss (82) provided convincing evidence of a decrease in force per crossbridge by observing a decrease in fiber stiffness relative to the force production of the fiber (82). In these experiments, the crossbridges were held in rigor by excluding ATP from the fiber bathing solution, and then the fiber was exposed to fast, sinusoidal changes in length so that both force and stiffness could be measured. From these experiments, one could conclude that force per crossbridge is decreased in the presence of acidosis. One confounding factor of these observations is that the changes in stiffness observed with acidosis are assumed to have occurred due to alterations in myosin's mechanical characteristics, an assumption that ignores the fact that other proteins within a muscle fiber play crucial roles in fiber structure and stiffness. For example, titin is a large protein in muscle fibers that passively produces stiffness when a fiber is stretched and this stiffness is subject to the concentration of particular molecules, such as Ca^{++} (73). Titin

and other molecules are also sensitive to acidosis and could also therefore lead to the observed change in stiffness. To tease apart the direct effect on myosin, experiments that measure the strength of the crossbridge in the presence and absence of acidosis are necessary. Using a laser trap assay, others have performed such experiments, but only in the absence of acidosis (89, 90). Here, once a single actomyosin crossbridge was formed in the absence of ATP, the actin filament was pulled to apply a resistive load to the myosin molecule. Because the laser trap acts as a spring, the farther the assembly is pulled the more force is applied to the myosin, and the force at which the actomyosin bond ruptures is recorded. These experiments are therefore feasible to do and could provide evidence of the effect of acidosis on the force per crossbridge. If acidosis reduces the force per crossbridge, the actomyosin bond should rupture at lower forces than in the absence of acidosis. Again, this would provide a direct observation and quantification of one of the putative effects of acidosis on myosin function.

To summarize our current understanding of the crossbridge cycle, myosin is the molecular motor in muscle that cyclically binds to actin to produce force and motion. The faster myosin moves through the crossbridge cycle, the faster muscle will contract, and the more myosin bind to the thin filament, the more force is generated. Despite what we know about myosin's crossbridge cycle, we do not have a complete picture of how the regulatory proteins and Ca^{++} affect myosin kinetics. We also don't know how multiple myosins work together to activate the thin filament. What follows is an explanation of the thin filament regulatory proteins, how they regulate actomyosin binding, and how the thin filament is activated. We then describe how specific perturbations affect this activation.

Finally, we discuss what gaps exist in our knowledge, and possible experiments that could help us fill those gaps.

Thin Filament Regulatory Proteins

Thin filament activation is required for a muscle to produce force and motion. During muscle activation, Ca^{++} is released into the cytosol of the muscle cell and allowed to bind to troponin. This leads to a slight structural movement of tropomyosin, a filamentous protein wrapped around actin. Together, troponin and tropomyosin are the regulatory proteins, so called because they regulate myosin's ability to bind to actin. During muscle activation, the shift in tropomyosin exposes myosin binding sites on actin, allowing myosin to strongly bind to the thin filament and subsequently produce force and motion.

Troponin has three subunits: the Ca^{++} binding subunit (TnC), the inhibitory subunit that binds to actin (TnI), and a subunit that is bound to tropomyosin (TnT). TnC is shaped like a dumbbell with eight major helices, labeled A-H (figure 2.2). The first four of the helices, A-D, are near the N-terminus and make up one of the ends of the dumbbell. The N-terminus is responsible for binding Ca^{++} during activation which subsequently causes a subtle movement of the helices B and C where they 'swing' away from the helices

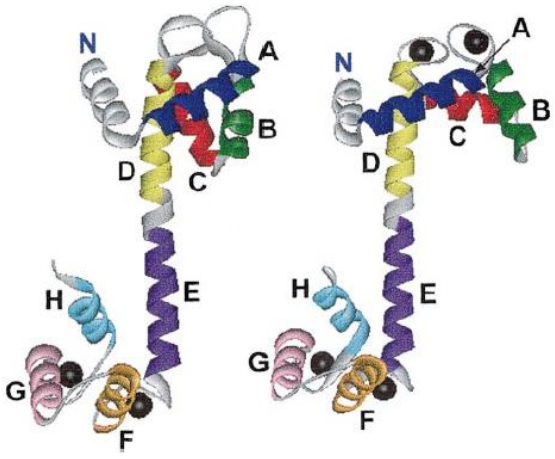

Figure 2.2. Structure of TnC. Helices are labeled A-H, from N-terminus to C-terminus. The subtle movement of the N-terminus is a crucial part of thin filament activation. From Herzberg and James 1985 (54).

A and D. This movement of the B and C helices exposes a hydrophobic patch on TnC where TnI can bind.

TnI does not inhibit actomyosin binding directly; rather, TnI anchors tropomyosin over myosin-binding sites on actin with its long C-terminus tail binding to actin. The C-terminus tail has two particular segments crucial for its function: the inhibitory sequence that binds to actin (residues 96-116) and the regulatory sequence (also called 'switch' sequence) that binds to TnC upon Ca^{++} activation (116-131) (44). Upon Ca^{++} binding and the subsequent movement within TnC, the regulatory sequence swings up and binds to the hydrophobic patch on TnC (figure 2.3). With the C-terminus of TnI now detached from actin, tropomyosin is no longer anchored to actin and can move on the actin surface, which can expose myosin binding sites. In summary, the intricate motions of TnC and TnI control tropomyosin movement which subsequently dictates myosin strong binding and thus the activation of the thin filament.

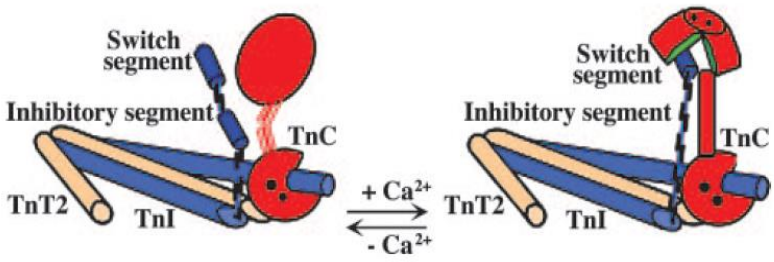

Figure 2.3. Structure of TnI. The C-terminus of Troponin I binds to actin in the absence of Ca++, but binds to TnC in the presence of Ca++. Figure from Vinogradova 2005 (123).

The function of TnC and TnI may be altered during muscle fatigue. During muscle fatigue, Ca^{++} levels may drop. In a rested, unfatigued muscle, Ca^{++} levels can be high enough to saturate troponin. However, as fatigue ensues, the pCa level can decline to approximately pCa 6 (71). This concentration is not adequate to saturate troponin and may lead to submaximal forces. In addition, acidosis may impede the function of TnC

and TnI. To tease apart which troponin subunit is most altered, chimeras of troponin were created, where troponin subunits from both cardiac and skeletal fibers are isolated and then mixed. For example, one chimera created in these experiments is TnC from cardiac fibers combined with TnI from skeletal fibers. The results from these experiments suggested that both troponin subunits are effected by acidosis, but TnC seemed to be the most sensitive (6, 30, 86, 93). Further work showed that the first 41 residues of both cardiac and skeletal TnC are responsible for this sensitivity (30). Further evidence of the effect of acidosis on TnC was provided by isolating TnC and examining its ability to bind Ca^{++} in the presence or absence of acidosis. The percentage of Ca^{++} bound to troponin was measured at various Ca^{++} concentrations, and acidosis led to less Ca^{++} binding across these Ca^{++} concentrations (93). Thus, an acidosis-induced reduction in thin filament activation likely occurs due to direct effects of acidosis on TnC. Considering that the first 41 amino acids play a crucial role in TnC function, in the presence of acidosis, the hydrogen ions may compete with Ca^{++} for the Ca^{++} binding sites on TnC (7, 8, 35).

Despite the evidence to suggest that acidosis predominantly affects TnC, some data shows that the effect on TnI is more important (22, 24, 131, 133). Cardiac Tn is more sensitive to acidosis than filaments with skeletal Tn, shown by a larger shift in the pCa-force relationship (86). More specifically, slow skeletal fibers are less sensitive to changes in pH, and this difference was hypothesized to be due to differences in TnI. Experiments showed that replacing cardiac TnI with slow skeletal TnI resulted in an attenuation of the effect of pH on cardiac fibers (131). By examining the amino acid sequence of these TnI isoforms, the authors focused on one particular amino acid that was different in the C-terminus. This amino acid is located at the 132^{nd} residue on

skeletal TnI and the 164th on cardiac TnC, which means this residue is located in the inhibitory region of TnI, a crucial part of the subunit that binds to TnC's hydrophobic pocket when the Ca^{++} is bound. Therefore, this is an area that plays a large role in the protein's function. To test this, TnI was engineered where this one amino acid was switched in both TnI isoforms and found that this caused slow skeletal fibers to be more sensitive to acidosis (133) while cardiac fibers were much less sensitive to acidosis (22). Interestingly, this one residue cannot account for all of the difference in acidosis sensitivity across fiber type. This can be ascertained by carefully examining the TnI amino acid sequence for slow skeletal, fast skeletal and cardiac fiber types. Both slow and fast skeletal TnI have this 'acidosis resistant' residue, yet fast skeletal TnI is significantly more sensitive to acidosis than slow skeletal TnI. Thus, this one residue does not save fast skeletal TnI, and thus other residues or structures in Tn must account for this acidosis sensitivity. Further work is necessary to find which residues are responsible for these differences. Regardless of the precise mechanism, these chimera and single point mutation experiments have provided the framework as to how the effects of acidosis can be attenuated.

Ca^{++} Activation of the Thin Filament

Ca^{++} activation dictates force and velocity production. During a maximal contraction in a fresh, unfatigued skeletal muscle, Ca^{++} levels are relatively high: almost all of the troponins will have Ca^{++} bound at any given moment, assuming a binding constant for Ca^{++}-Tn of ~ 0.5 µM (93). This allows tropomyosin to move freely on the actin surface, and allows myosin to bind to the thin filament. However, there are some important cases where Ca^{++} levels aren't at maximum levels. One example is during

muscle fatigue, where during prolonged intense contractions, Ca^{++} levels in the cytosol drop (3, 130). This leads to a decrease in filament activation and thus a decrease force and velocity. Another example of submaximal Ca^{++} levels during contraction are those experienced in cardiac muscle. In each cycle of contraction and relaxation that occurs with a heartbeat, maximal Ca^{++} levels are never reached. This means that during successive heartbeats, the Ca^{++} concentration quickly slides up and down the steep portion of the pCa-force relationship. As shown before, a typical pCa-dependent relationship is shown in figure 1.3.

These data are fit to the Hill equation, shown here:

$$y = \min + \frac{\max - \min}{1 + 10^{\log(pCa50 - pCa)n}}$$

Where 'min' equals the minimum velocity, 'max' is the maximum velocity, 'n' is the Hill coefficient, and pCa_{50} is the amount of Ca^{++} necessary to reach half-maximal velocity.

The first major outcome is the pCa_{50}. The Ca^{++} concentration required to elicit half-maximal velocity or force is termed pCa_{50} and is a measure of Ca^{++} sensitivity. A lower pCa_{50} suggests more Ca^{++} is necessary to reach a given velocity or force; conversely, a higher pCa_{50} suggests less Ca^{++} is necessary. Ca^{++} sensitivity is important considering how steep the pCa-velocity and pCa-force relationship are: subtle changes in the Ca^{++} concentration can drastically change work output of a muscle. Perturbations within the muscle cell, drastically alter this relationship, where much more Ca^{++} is necessary to reach a given force output (88). A possible method to examine the effect of such perturbations on Ca^{++} sensitivity is to use the laser trap assay to directly observe myosin interact with a regulated thin filament across a range of Ca^{++} levels. This can also be done with a small ensemble of myosin interacting with one regulated actin filament.

This would recapitulate *in vivo* muscle, as many myosins work together to pull on a regulated actin filament.

The second major outcome from a pCa-force relationship is the cooperativity of myosin molecules. The Hill coefficient, *n*, is an indication of this cooperativity. When $n > 1$, binding is said to be cooperative, where one binding event accelerates the rate of subsequent binding events (45). In the case of the contractile proteins, this suggests that one myosin binding event facilitates subsequent myosin binding. Cooperativity has four main mechanisms: 1) coupling between the two Ca^{++} binding sites on fast skeletal TnC, 2) coupling between Ca^{++} binding sites down the thin filament, 3) myosin strong binding inducing Ca^{++} binding to TnC, and 4) myosin strong binding inducing movement of tropomyosin into an open state so other myosin can more easily (44).

There is some evidence for the first mechanism contributing to cooperativity, though not by much. There is evidence that the two Ca^{++} binding sites on fast skeletal TnC bind cooperatively, leading to a Hill coefficient of 1.2 (46). This mechanism isn't possible in cardiac TnC, which only has one Ca^{++} binding site. Interestingly, if skeletal TnC is added to cardiac thin filaments, cooperativity is observed (4). Regardless of this cooperativity, the first mechanism of cooperativity is not enough to explain the highly cooperative action observed in fibers.

There is also evidence for the second mechanism, where Tn along the thin filament are able to cooperatively bind Ca^{++}. By using fluorescent probes on Tn, Ca^{++} was shown to bind cooperatively down the thin filament (46, 50). Other experiments suggested this mechanism of cooperativity by performing partial extractions of TnC and observing cooperativity decrease (10, 87).

Like the first two mechanisms, the third mechanism likely plays a small role, but there is evidence that myosin binding can cooperatively increase Ca^{++} binding to Tn, Experiments using fluorescent probes on Tn (50) suggest that Ca^{++} binding to Tn is influenced by myosin. Other experiments have tested this hypothesis using myosin modified with BDM, which keeps myosin in a weakly bound state (93). However, some have suggested that only rigor myosin have this effect, which leads to the question if this mechanism would occur under physiological conditions (11, 39).

The fourth mechanism is most likely to have the biggest effect in generating cooperativity and thus Hill coefficients greater than 1.5. This has been demonstrated multiple times by either decreasing ATP or by increasing ADP (40, 48, 56, 104). The former would increase rigor myosin, while the latter would increase M.ADP myosin, both of which can strongly bind to the regulated thin filament and help neighboring myosin to bind. Similarly, NEM modified myosin were used to activate the thin filament (111). Additional evidence for the fourth mechanism comes from experiments with partial TnC extractions: by removing TnC, the tropomyosin stays in the blocked state and prevents myosin from communicating. Finally, creative experiments were done with fluorescent S1 myosin, which were observed binding to a native myofibril. S1 bound to the overlap region (of the thick and thin filament) four times more than the nonoverlap region, suggesting that the myosin in the thick filament helped the fluorescent S1 bind to the overlap region. These experiments were done with both rigor and M.ADP S1 under high Ca^{++} and low S1 conditions. To further support myosin-myosin cooperativity, as S1 was increased in this experiment, the S1 would bind to the nonoverlap region in highly cooperative manner (112). Thus, there is a large amount of evidence to suggest that

myosin-myosin cooperativity is the biggest contributor to the highly cooperative nature of the pCa-force relationship.

How cooperativity occurs is a dynamic and complex process and has been difficult to characterize. Indeed, recent innovative approaches (29) and sophisticated mathematical models (42, 84, 126) have tried to describe this phenomena quantitatively. Why is it difficult to quantify and characterize cooperativity? This is because cooperativity involves both elements of time and space, where myosin binding to actin is short-lived (as short as 2 ms) and thus only activates the filament for a very short period, and will only facilitate binding of other myosins that are nearby. Why is myosin necessary to activate the thin filament? Previous work (52) suggested that tropomyosin worked like a switch that could either be open, allowing myosin binding, or blocked, preventing myosin binding. An alternative hypothesis suggests that tropomyosin explores three states: blocked, closed, and open. In both models, tropomyosin blocks actomyosin binding sites in the absence of Ca^{++}. In the latter model, called the three-state model, Ca^{++} binding does not cause tropomyosin to completely open the actomyosin binding sites; rather, it only slightly exposes them, and so this state is called the closed state. Finally, when a myosin binds to actin, myosin pushes the tropomyosin to the open state. An important note is that tropomyosin is dynamic, and that even in the absence of Ca^{++} tropomyosin has a finite probability of being in the open state. For example, previous work has quantified this probability, showing that even in the presence of Ca^{++}, tropomyosin is in the closed state 75% of the time while it is in the open state 98% of the time when myosin binds to actin (45, 81). This three state model is further supported by

biochemical experiments (72, 81, 118), *in vitro* motility assay (62), fiber studies (111), modeling (62, 81), and structural studies (19, 98, 108, 122, 125). Clearly, actomyosin binding plays a crucial role in thin filament activation, but how does this effect other myosin molecules? When one myosin pushes tropomyosin into the open state, this state is propagated down the thin filament, where other actin monomers now have their binding sites more exposed. To understand cooperativity, the distance down the filament that tropomyosin movement is detected is a crucial measure. This, of course, depends on how rigid tropomyosin is: if tropomyosin is rigid like a metal rod, when one myosin binds to actin the whole tropomyosin structure should be pushed to the open state. On the other hand, if tropomyosin is soft and flexible, the open state may not even propagate down the tropomyosin molecule for the next myosin. In reality, the data suggests that tropomyosin is semi-rigid: experiments using the laser trap assay have shown that one myosin binding can facilitate another that is approximately 110 nm away (62). However, other work has shown that tropomyosin may be more flexible than previously thought, as determined by its persistence length (77). Persistence length is a common measure of the stiffness of filamentous proteins, where pieces of the beam that are closer together than the persistence length are correlated and represented as part of a semi-rigid rod, while pieces

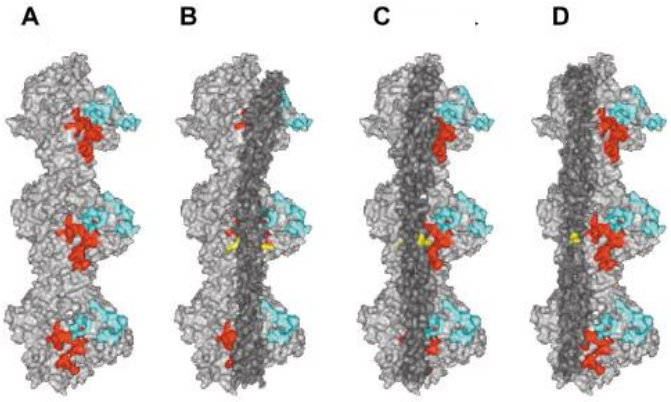

Figure 2.4. Cartoon of the 3-state model of thin filament activation. Actin (light gray) and tropomyosin (dark gray) in the blocked (B), closed (C), and open (D) state. Areas on actin where myosin binds weakly (green) and strongly (red) are highlighted. Figure from Gordon et al. 2001 (45).

farther apart than this threshold are not correlated. Previous findings suggest that tropomyosin's persistence length anywhere from 40-500 nm (62, 77, 80, 97, 103, 122). Such various values make determining how far cooperativity is propagated down the thin filament quite difficult. Furthermore, neither the term 'persistence length' or 'cooperative length' capture the physiological complexity of cooperativity. Are all myosins within this distance treated equally? For example, if the cooperative length was 100 nm, do both the myosin 10 nm away and the myosin 90 nm away increase their chances of strong binding to the thin filament? Or is the probability of a second myosin binding increased if it is closer to the first myosin that is bound? Sophisticated mathematical models of thin filament activation suggest the latter (126, 127), but experimental data with small ensembles of myosin are necessary to confirm this, especially in the presence of submaximal Ca^{++} levels. Such experiments would provide crucial information on how both Ca^{++} and myosin strong binding play a role in thin filament activation. Additional experiments in the presence of acidosis can explore this effect on cooperativity.

To successfully model thin filament activation and subsequent muscle output, a universal model must 1) take into consideration many sets of data and be able to match the data, 2) explain and match data across all scales of muscle, from the whole organ to the single myosin, 3) be within the limits of current computational power, and, of course, 4) explain data across different activation conditions, such as various Ca^{++} levels, various myosin concentrations, and various metabolite concentrations, such as ATP, P_i, etc.

Some models use Monte Carlo simulations to predict behavior on a sarcomere level (14). This model is able to describe activation, even at low Ca^{++} levels (1). Unfortunately, Monte Carlo simulations are computationally heavy, and can only model

small parts of muscle (in this case, one thin filament). Further, this model has not been tested in its ability to explain whole muscle findings or data with metabolic perturbations.

Other models are designed to explain whole muscle findings using molecular inputs. For example, Tanner et al. developed a model that recapitulates the lattice structure of muscle (116). They argue that this 3D model is better than a comparative 2D model. Though informative, this model has also not been tested with metabolic perturbations. In addition, a minor critique is that rate constants used in the paper come from three different research groups. These rate constants were determined from myofibril or muscle fiber data. Though reliable, these data are not determined through direct observation. On the other hand, data collected from assay such as the laser trap assay are from direct observation and can provide the most reliable picture of the actions of thin filament activation on the molecular level.

Though many models exist, the model that seems to fit all of our criteria is created by Walcott (126). This model has been tested with many sets of data across the scale of muscle, especially with single molecule and small ensemble data sets (28, 62, 127). A large benefit of this model is that this model uses findings from a specific cohort of researchers (28, 62, 128) which ensures fidelity. This model uses the more computer friendly partial differential equations (PDEs) to perform calculations, as opposed to Monte Carlo simulations, which, while useful, can be computationally heavy because they aim to characterize each molecule's behavior at any given moment. Finally, and possibly most important, this model can make predictions across all muscle scales, from the single myosin molecule up to whole muscle.

The R146G Mutation

A major goal of this work is to better characterize thin filament activation so that we can apply that knowledge to muscle fatigue or diseases caused by point mutations. A key way the knowledge can be applied is to compare the molecular details of activation under normal conditions to situations that arise with mutated proteins. This is particularly relevant to cardiac muscle, where a single point mutation can disrupt normal activation, leading to abnormal force production and many times leading to lethal cardiomyopathies (79). The most common mutations that lead to such drastic outcomes occur in the sarcomere, including myosin, myosin binding protein C, tropomyosin, or troponin (79). While the many common mutation sites within these three proteins are actively being studied, one in particular, the R146G mutation in TnI, has been a quagmire and may affect both myosin kinetics and Ca^{++} binding dynamics (12, 34, 60, 69, 70, 75, 114, 129, 132, 138). Considering this, we felt this particular mutation was worth examining further.

Cardiac Troponin Structure

Cardiac troponin is slightly different than the skeletal isoform discussed earlier. The two major differences are that cardiac troponin C has only one Ca^{++} binding site on the N-terminal, and that cardiac troponin I has 30 more amino acids in the N-terminal. These 30 more amino acids cause a shift in the homologous structures. For example, the inhibitory region of skeletal troponin I is located near amino acids 96-116, while the inhibitory region of cardiac troponin I is located near amino acids 126-146. These places our mutation of interest within the inhibitory region of cardiac troponin I. This particular mutation involves a switch from a relatively large, charged arginine to the small, hydrophobic glycine. Exactly how this alters the structure of TnI is difficult to say. As

some have pointed out, many cardiomyopathic mutations are clustered in flexible regions of proteins, which makes obtaining structural data with cryo-EM or crystallography quite difficutl (12). This flexibility may lead to the mutation's negative effects on myosin and thin filament activation.

Effect of R146 on Myosin

Interestingly, the R146 mutation seems to affect myosin's function, even at maximal Ca^{++} activation. At maximal Ca^{++}, myosin binding is expected to be the limiting factor in force production (41). Yet, with this mutation, there is evidence that force is reduced at maximal Ca^{++} (70, 129). Interestingly, these results are equivocal, where others have shown no significant decline in force (114, 132). The discrepancy may be due to differences in expression of the R146G mutation across transgenic experiments. James et al showed that differences in expression level can alter the phenotype (60). Specifically, mice that expressed a larger percentage of R146G relative to wild-type troponin had a lower survival rate. The cause of the observed reduced force in (70, 129) is difficult to explain, considering high Ca^{++} levels should fully activate troponin and tropomyosin, and any limit in force would be due to a limit in myosin kinetics or mechanics. Indeed, some have proposed that the R146G alters myosin's crossbridge force (129). This is surprising, as TnI interacting with or altering myosin's function is unexpected. Others have found that the cause and effect relationship is different: using FRET, Zhou (138) measured the Ca^{++} dependence of the TnC-TnI interaction in both wild-type and R146G filaments, and found that the presence of S1 myosin induced a large shift in the pCa_{50} in mutant filaments but not in wild-type. These data suggest that S1 somehow influences TnC-TnI dynamics in the presence of the R146G mutation.

In addition to a decline in force, the mutation causes a decline in ATPase activity at maximal Ca^{++} (70, 114), though others have found no decline in this measure (34, 129). The discrepancy in results does not seem to be due to differences in methods, considering Lang et al. 2002 and Elliot et al. 2000 both used reconstituted thin filaments in solution.

Finally, the R146 mutation has been shown to reduce peak velocity at maximal Ca^{++} in a motility assay (12) but not in fiber assay from transgenic mice (60). Here, the difference could be attributed to the overall percentage of R146G troponin. In a motility assay, the percentage of any given protein can be easily controlled (in this case, 100% of the troponin in the regulated thin filaments was mutated) while transgenic models rarely achieve 100% inoculation. Though the percentages achieved in James 2000 (40-80%) are a better representation of the expression levels in patients with this cardiomyopathy, the decline in motility shown in Brunet et al. provides insight into how this mutation affects force and motion. Brunet et al. propose a model where the R146G mutation contributes to a very flexible TnI subunit. The result is incomplete inhibition of actomyosin binding in the absence of Ca^{++} and incomplete activation upon Ca^{++} binding, suggesting the mutation does not affect myosin directly.

Effect of R146 on Thin Filament Activation

The more obvious effect of a mutation in troponin is the effect on Ca^{++} sensitivity. Indeed, the R146G mutation leads to an increase in the Ca^{++} sensitivity, indicated by an increase in the pCa_{50}, in ATPase measures either in solution (34, 114) or in isometric fibers (129). Similar shifts in the pCa_{50} have been found in isometric force measures of fibers from transgenic mice, transfected mice, and in fibers following a Tn exchange that

contained the R146G mutation (60, 70, 114, 129, 132). However, there is data showing that the R146G mutation has no effect on force in transgenic mice or following Tn exchange (69). Finally, the shift in Ca^{++} sensitivity has recently been seen in the pCa-velocity relationship as well (12). In addition to finding an increase in Ca^{++} sensitivity, many have found that the R146G mutation is not sufficient to completely inhibit ATPase at low Ca^{++} (34, 70) nor is it sufficient to completely prevent force production (69, 70, 114, 129).

What can explain the overall findings for the R146G mutation? How does this mutation leads to enhanced ATPase and force at low Ca^{++} but reduced ATPase and force at high Ca^{++}? One model suggests that the R146G mutation leads to weaker bonds to both actin (34) and to TnC (75). A weaker bond to actin under low Ca^{++} conditions would increase the probability of TnI detaching from actin, allowing tropomyosin to move on the actin surface and eventually will lead to a higher probability of myosin binding to actin. A weaker bond to TnC, on the other hand, would lead to a lower probability of TnI binding to TnC upon Ca^{++} activation. This may suggest that TnI is moving freely or TnI may still be bound to actin, despite the presence of Ca^{++}. Another possibility is that the mutated TnI interacts with myosin under high Ca^{++} conditions. As stated earlier, this interaction seems unlikely but there is evidence to suggest that the mutated TnI affects myosin's crossbridge force. If this TnI-myosin interaction is possible, the mutated TnI may not only myosin's mechanics, but also its kinetics. More specifically, experiments examining the effect of the mutation on myosin's on-rate as well as myosin's duty cycle would add to our understanding of this mutation. While determining the precise structure

and dynamics of R146G TnI is very difficult, determining how the mutation affects myosin kinetics can be easily examined in an *in vitro* motility assay.

CHAPTER 3

METHODS

To achieve the aims of this project, the laser trap assay and the *in vitro* motility assay were used. As alluded to before, *in vivo* studies as well as single muscle fiber and motility experiments have led to our current understanding of working muscle. Though informative, more precise techniques are needed to understand the molecular basis of thin filament activation and muscle contraction. To achieve this, the laser trap can be used to examine the molecular details of the contractile proteins. Single muscle fibers contain billions of myosin molecules as well as a complex array of other proteins, but the laser trap assay allows for the direct observation of a single myosin molecule interacting with a single actin filament. Here, we can directly observe specific steps of the crossbridge cycle, a feat not achievable with muscle fibers. The laser trap assay can be used to better understand actomyosin binding kinetics, force production of single myosin molecules, and activation of the regulated thin filament (5, 15, 25, 29, 37, 62, 121). The laser trap assay was used to directly observe, on the nanometer and millisecond scale, the binding and force-producing capacity of an individual and small ensembles of myosin.

Using this assay, we first examined the effects of Ca^{++} on a single myosin's ability to bind to a regulated thin filament. We measured the binding events per second as well as each event's duration. Second, we examined how a small ensemble of myosin interact with a regulated thin filament. We directly observed the how a small ensemble of myosin work together in a cooperative fashion to pull on the actin filament to generate force and motion in a Ca^{++} dependent manner. These experiments enabled us to recapitulate the pCa-force relationship on the molecular level. In addition, this particular

experiment was one of the best representations of *in vivo* muscle because of our use of a small ensemble at relatively high (100 μM) ATP concentrations.

The *in vitro* motility assay is designed to observe unloaded velocity of actin filaments as they are propelled by myosin in a variety of conditions. In our experiments, we manipulated ATP and Ca^{++} and measure the resulting velocity. This technique, called a "rigor activation" assay, will provided insight into thin filament activation. This is because Ca^{++} affects regulatory protein dynamics, while ATP affects myosin's kinetics, in particular, how long myosin stays bound to actin in the rigor state. Because both Ca^{++} and myosin strong binding play a role in thin filament activation, this assay provides insight into the dynamics of each.

We also used the *in vitro* motility assay to examine the effects of a particular troponin mutation, R146G, on thin filament activation and myosin kinetics. To examine these effects, we first measured unloaded velocity in a Ca^{++} dependent manner and generated a pCa-velocity relationship. We then performed a duty cycle experiment, where the number of myosin heads available to the regulated thin filament was manipulated and the velocity of each filament was measured. These data were then fit to a duty cycle equation (120):

$$V = V_{max} * (1 - (1 - f)^N)$$

to determine the percentage of time myosin is strongly bound to the filament. In this equation, V is the measure velocity of a filament, V_{max} is the maximum velocity, f is the duty ratio, or the percentage of time myosin is strongly bound to actin, and N is the number of myosin heads interacting with the filament. As V changes as a function of N, and the data can be fit, where V_{max} and f are determined by the fit. Finally, we then

manipulated ATP in a motility assay to examine if the R146G mutation alters myosin's ADP-release rate, which directly affects myosin's on-time.

Overall, the proposed experiments have allowed a better understanding of the molecular details of thin filament activation. The experiments also provide insight into how thin filament activation is altered by troponin mutations. This will set a foundation for future work that can examine this mutation and others that lead to cardiomyopathies and the development of therapeutics to combat the negative effects associated with the mutations.

Laser Trap Assay

Background

The laser trap assay was used to directly observe either single myosin or a small ensemble of myosin generate force and motion by interacting with a thin filament. To do

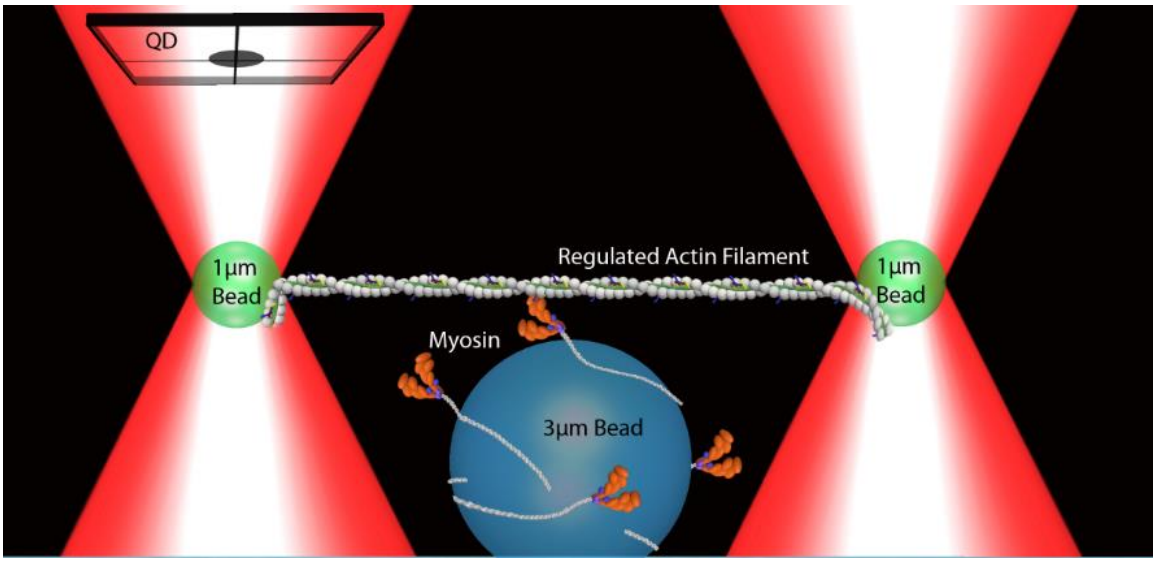

Figure 3.1. Cartoon of the 3-bead assay. Myosin is randomly oriented on the microscope slide surface, occasionally located on a pedestal bead. A bead-filament-bead assembly, trapped by laser light, is put in close vicinity to the pedestal so single molecule interactions can be observed and measured. Figure courtesy of Mike Woodward.

this, a powerful, densely focused beam of light traps two 1 µm glass beads which are then attached to each end of a thin filament. This bead-filament-bead set up, or "dumbbell" set

up, is positioned near a 3 μm bead on the microscope slide surface that is sparsely coated with myosin (figure 3.1). This set up enables one myosin molecule or an ensemble of myosin molecules to interact with the actin filament. As myosin pulls on the thin filament, the position of one bead is detected by a quadrant photodiode, which can discern nanometer and millisecond motions, and the force exerted on the filament by the myosin can be calculated.

Hardware and Software

The optical light path used to form the laser trap is very similar to that previously described (28) with minor changes. Briefly, a 5 W, infrared (1090 nm) laser beam (SPI Lasers, Santa Clara, CA) is timeshared between two locations at 10 kHz using two orthogonally (x and y) oriented acousto-optic deflectors (AODs) (DTD-274HA6, Intra Action, Bellwood, IL). An AOD serves to deflect a beam of light as a function of the radiofrequency transmitted through the medium. By altering the frequency, the beam of light and thus the trapped bead can be steered. The AOD is driven by a custom-built digital controller (Elliot Scientific, Hertfordshire, United Kingdom) that interfaces with a personal computer via a field-programmable gate array card (PCI-7830R, National Instruments, Austin, TX) and custom software developed using the real-time module of LabView version 8.6 (National Instruments).

Displacements of one of the trapped beads were determined by imaging the interference pattern of the bead onto a quadrant photodiode (QD) (G6849, Hamamatsu Photonics, Hamamatsu City, Japan) conjugate with the back focal plane of the condenser (32). This displacement signal was digitized via a National Instruments data acquisition module (USB 9162) and collected at 5 kHz. Coarse movements of the microscope stage

were made using a manual micrometer-driven stage with a capacitive servo-feedback piezoelectric substage (Nano-Bio200, Mad City Labs, Madison, WI) that can generate nanometer movements for fine control. The fluorescent thin filament was then visualized using an intensified CCD camera (Stanford Photonics, Palo Alto, CA) while simultaneously visualizing the silica beads in bright field using a CCD camera, which interfaced with the PC.

Trap Stiffness Calibration

The force of the laser light applied to a 1 µm bead behaves as a simple linear spring, where F = k * x, where F is the force, k is the spring constant of the trap (or stiffness) and x is the distance the bead is from the center of the trap. The stiffness of our optical trap was determined two different ways: the equipartition method and the power spectral density method. The equipartition method relies on the relationship between thermal energy and the spring energy. The thermal energy for one-dimensional diffusion is $\frac{1}{2}k_BT$, where k_B is the Boltzmann constant and T is the temperature of the environment. The spring energy of a bead in an optical trap is $\frac{1}{2}kx^2$, where x^2 is the variance in the bead's position. Therefore, we can derive:

$$k_{trap} = \frac{k_B * T}{x^2}$$

We measured the variance of the bead's position and determine the stiffness of the trap. To confirm our calculations, we used the power spectrum density. For a sphere in solution, the drag coefficient, γ, is calculated as:

$$\gamma = 6 * \pi * n * r$$

Where *n* is the viscosity of the solution and *r* is the radius of the bead. The power spectral density gives the function:

$$F(t) = \frac{k_B * T}{2 * \pi^2 * \gamma * (f^2 + fc^2)}$$

Where *fc* is the corner frequency, which is equal to:

$$fc = \frac{k_{trap}}{2 * \pi * \gamma}$$

And thus, the stiffness of the trap, k_{trap}, can be calculated.

Proteins

Whole myosin and actin were purified from chicken pectoralis muscle based on previous methods (78, 92). SDS gels and High Performance Liquid Chromatography (HPLC), tools used to separate proteins by size and charge, demonstrated the high purity of the proteins. Myosin was stored in glycerol (50% v/v) at -20°C for up to 1 year. The purified actin filaments were fluorescently labeled and stabilized with TRITC/phalloidin and coated with biotin and stored at 4°C. Wild-type skeletal troponin was purchased (Life Diagnostics, West Chester PA), while troponin variants will be generously provided by our collaborator Dr. Tomo Kobayahsi at the University of Illinois. Dr. Tomo Kobayashi prepared and provided troponin as described here. Recombinant mouse cardiac TnI, TnC, and TnT was inserted into pET3d vector and expressed using BL21(DE3) cells. Expression of the correct sequence was confirmed by DNA sequencing. The subunits were purified, reconstituted, and frozen in liquid nitrogen. The troponin variants were divided into single experiment sized aliquots, snap frozen in liquid nitrogen, and stored at -80°C until the day of the experiment.

Solutions

On the day of an experiment, the purified chicken pectoralis myosin was diluted to 200 μg/mL in myosin buffer (300 mM KCl, 25 mM Imidazole, 1 mM EGTA, 4 mM

MgCl2, 1 mM DTT). An equimolar concentration of purified chicken pectoralis actin was added to this solution, in addition to 1 mM ATP. This solution was centrifuged at 400,000 g for 20 minutes to separate live myosin from 'dead-head' myosin that cannot hydrolyze ATP. The 'dead-head' myosin bind to the actin and pellet, while the live myosin stays in solution. This solution was extracted and diluted so the myosin was at a final concentration of 0.1 µg/mL for single molecule experiments or 10 µg/mL for experiments with small myosin ensembles.

To create reconstituted regulated thin filaments, on the day of an experiment 1 µM actin was mixed with 0.25 µM troponin and 0.25 µM tropomyosin and allowed to incubate for 3 hours. This solution was then diluted to bring the actin concentration to 10 nM. Full reconstitution and thus full regulation was confirmed by performing an *in vitro* motility assay with 100 µg/mL myosin and the regulated filaments at pCa 10. After the 3-hour incubation, the actin was diluted in a low salt actin buffer (25 mM KCl, 25 mM Imidazole, 1 mM EGTA, 4 mM MgCl2, 1 mM DTT) to 10 nM. BSA was diluted in actin buffer to 0.5 mg/mL. The 1 µm trapping beads were incubated with 0.5 mg/mL neutravidin and allowed to incubate for 3 hours. After 3 hours, the beads were diluted in actin buffer and sonicated to remove excess neutravidin that did not bind tightly to the 1 µm beads. This washing process was repeated and the beads were then diluted in 500 µL of actin buffer.

The final buffer for the laser trap assay was composed of actin buffer with experiment-specific additions. For pCa-force experiments, a calculated amount of Ca^{++} was added to reach a specific Ca^{++} concentration and 100 µM of ATP was used. For single molecule binding experiments that examine on and off rates, 10 µM of ATP will

be used. For all experiments, the ionic strength was held constant at 95 mM by adjusting the amount of KCl added to the final buffer. The pH of the final buffer was set to 7.4. Buffer recipes will be determined using a computer algorithm with known chemical binding constants, with adjustments for temperature, pH and ionic strength (WinMaxC) (52). All final buffers contained an oxygen scavenger system (1725 mg glucose, 75 mg glucose oxidase, and 14 mg catalase) to prevent photobleaching of the actin filaments.

Laser Trap Assay Protocol

Myosin was added to the flow cell and allowed to bind to the nitrocellulose-coated surface for 2 minutes. BSA was flowed in and allowed to incubate for 5 minutes to ensure actin does not attach to the nitrocellulose surface. While this incubation occurs, the neutravidin beads were sonicated to break apart any coagulation. 3 µL of the beads were added to 181 µL of final buffer. This aliquot was vortexed to ensure a homogenous mixture of beads. 8 µL of the 10 nM labeled actin and 4 µL of each regulatory protein at 5 µM was added to this final buffer. The flow cell was placed on the microscope. Finally, the final buffer was added to the flow cell.

In the flow cell, we trapped 2 of the 1 µm beads. A labeled, regulated, biotin coated actin filament was secured between these two glass beads. Once a bead-actin-bead complex was assembled in the laser trap, the filament was pulled taught, with a pretension of 4 pN. The complex was lowered to a 3 µm bead coated with myosin. As the QD determines the position of one of the neutravidin beads, actomyosin activity can be observed. Actomyosin activity is confirmed by a directional displacement of the bead from the laser trap, as determined by the QD. Once activity is observed, a 5 second recording was taken.

Data Analysis

The positional data of the 1 µm bead was measured in mV, which was converted to nanometers after an internal calibration. For the data collected with a small myosin ensemble, the data was then converted to forces, measured in pN, by multiplying the nanometer displacements by the stiffness of the laser trap. In this way, we determined the force produced by a small myosin ensemble.

To objectively detect single molecule events, an analysis called the Page method was used (66). Essentially, this method looks for a decrease in variance in the signal, which occurs when myosin strongly binds to actin. If this decrease in variance lasts long enough, the program detects it as an event. More specifically, the original signal is corrected to zero. The program then examines each point and calculates the probability of the data point being part of an event based on how far the point is from zero. If the probability is relatively high, a value is added to a cumulative sum, whereas each succeeding point that has a high probability will also add to the sum. Once this sum reaches a pre-determined threshold, the program

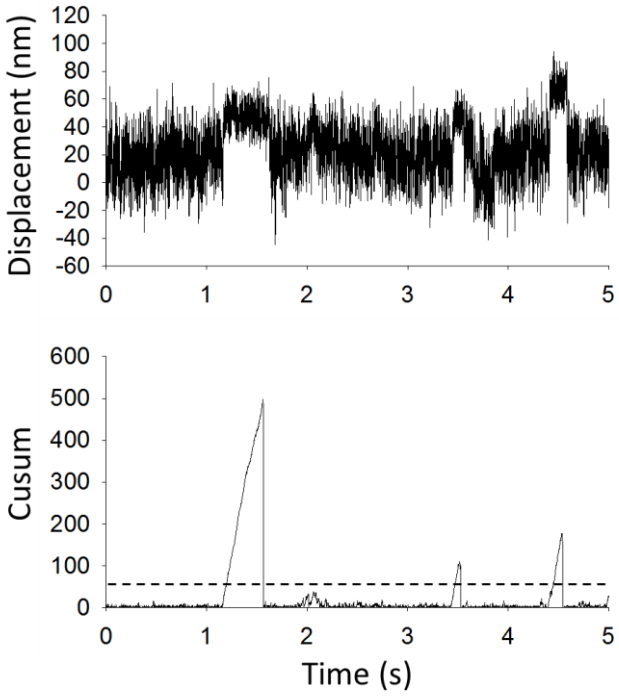

Figure 3.2. Example of the Page method. Single molecule recordings were examined using the Page Method. A sliding window is used to determine the variance of the window. A low variance will lead to a cumulative sum. An event is counted once the cumulative sum reaches a predetermined threshold.

recognizes the data points to be part of an event. A sample trace and the corresponding cumulative sum is shown in figure 3.2.

For force measurements with small myosin ensembles, each recording was analyzed with a custom Matlab computer program. A brief description of the program is as follows: first, the program examines all the data and determines the baseline of the trace, where myosin and the thin filament are not bound. The program then examines each data point in the file, checking if it is at least 8 nm above the baseline. The 8 nm threshold is based on previous literature suggesting that when myosin binds to actin, it generates a powerstroke that is at least 8 nm (15, 119). Therefore, this is the first criteria to see if myosin has bound to actin. This minimum 8 nm displacement must occur for 10 consecutive milliseconds for the program to determine that a binding event has occurred. The 10-millisecond criterion is based on the expected duration of a single myosin-actin interaction. This interaction is dependent on the length of the actin-myosin-ADP state and the myosin-actin rigor state. Assuming an ADP release rate of 100 to 350 per second (5, 128) and an ATP binding rate of 2 to 7 $x10^{6} * s^{-1} * M^{-1}$ (5, 91), approximately half of the single myosin-actin binding events should last 10 ms or longer at our experimental conditions of 100 μM ATP. Once the program determines that an event has occurred, the time at which the event began is determined. In addition, if this is not the first event in the recording, the program calculates how much time has passed since the previous event ended. This is a useful measure that provides insight into the binding frequency, a measure that is expected to change under the various conditions tested, particularly the different Ca^{++} concentrations. Finally, when the event has ended, determined when the recording has dropped back down to baseline, the duration of the event is calculated. In

addition, the program examines the event and finds the 10 ms region that contains the highest average mV signal. This average is then converted to pN and this peak force is recorded. Thus, overall, the program can determine when an event occurs during a recording, and then determines the duration and peak force of each event.

Some of our experimental conditions, including single myosin molecule experiments or conditions with low Ca^{++} (pCa 9), required a different analysis strategy. Under these conditions observing distinct single myosin-actin binding events in the recording is difficult. However, actomyosin binding significantly reduces the noise in the force recording (figure 3.3). This occurs due to the stiffness of the myosin-actin bound, which reduces the movement of the actin filament and thus the detected 1 µm bead. Again, an in-house Matlab program will examine the force recordings to determine when an event has occurred. This program is very similar to the one used for myosin ensembles, except instead of using an 8 nm displacement as a criterion, we will use a 70% drop in the variance of the signal. This cut-off was determined based on our current estimates of the myosin-actin stiffness of 0.3 pN/nm and the expected decrease in the variance based on this stiffness. Further, preliminary experiments have shown that this threshold works well, as data recordings showed events, while control recordings (ones where a recording was collected with the dumbbell set up positioned away from a 3 µm pedestal bead and therefore where no myosin-actin binding could occur) showed no

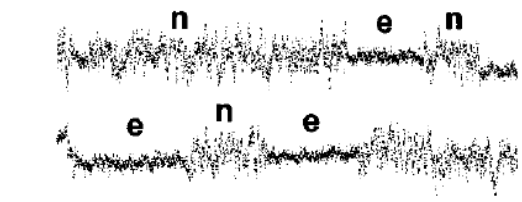

Figure 3.3. Example of capturing events with Brownian motion. During a recording, the signal of the 1um bead is noisy (n) but during a myosin-actin binding event (e) the variance drops significantly. Figure from Veigel and Molloy (121).

events. Though force measurements were not taken with this program, the duration and time between can be measured as before. Therefore, we can gain insight into the on and off rate of a single myosin molecule under many different conditions.

A critical measure for laser trap experiments is the height of the dumbbell set up relative to the pedestal bead. Knowing that the thin filament is close enough to the pedestal bead to allow myosin binding is important as this can affect the frequency of myosin binding; this value must be consistent from one condition to another. Therefore, during a recording we recorded a bright field image of the 3 µm bead. The height of the dumbbell set up was determined by analyzing the airy disc diffraction pattern of the 3 µm bead. This analysis can be used to determine axial position of micrometer particles (136). We have applied this technique to our microscope and took approximately 30 images at known heights, from 2.5 µm to 4.5 µm, and established a linear relationship between the airy disc radius and its height (figure 3.4). These heights were recorded by driving the 3D piezoelectric stage with nanometer resolution. A custom Matlab program was then written to calculate future images based on our standard curve. Testing the model with additional images at known heights showed that the model was accurate within 100 nm.

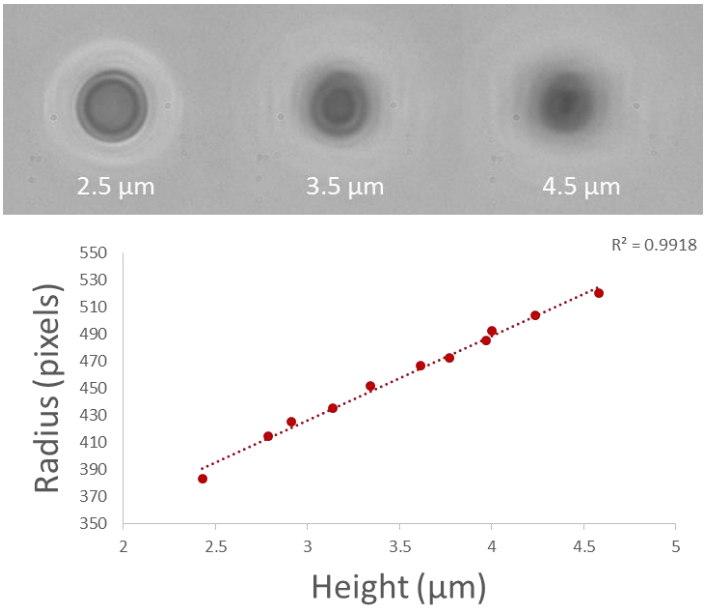

Figure 3.4. Determination of trap height. Top: Images taken of the 3 µm pedestal bead at different heights in the laser trap assay using a brightfield camera. Bottom: Calculating the airy disc created by the pedestal bead shows that the radius is linearly related to the z-position in the laser trap.

Our data collected at high Ca^{++} shows that heights up to 3.5 µm above the surface allow actomyosin binding, but heights above this do not. As stated earlier, some conditions resulted in very discrete and scarce events. Therefore, some data recordings may show no events at all, but if the corresponding height is within 3.0 to 3.5 µm, the data recording was considered in the final analysis. Conversely, if the file is collected above 3.5 µm, the data recordings were discarded.

Statistical Analyses

Histograms were generated for all experiments performed with a small ensemble of myosin, showing the relative frequency of forces, durations, or time between events. These measures were not normally distributed (28) and therefore a nonparametric Kruskal-Wallis analysis of variance was performed to identify significant differences across conditions, with differences identified using the method of Dunn (31).

For our experiments examining on and off rates of single myosin binding events we used a one-way ANOVA comparing the different pCa concentrations. All statistical procedures will be performed in SigmaPlot v11.0 (Systat Software, San Jose, CA) with the alpha level set at $p < 0.05$.

Mathematical Model

A major goal of this dissertation was to deconvolve the role of Ca^{++} and myosin strong binding during thin filament activation. To do this, we compared our single molecule binding results with our small ensemble results using a mathematical

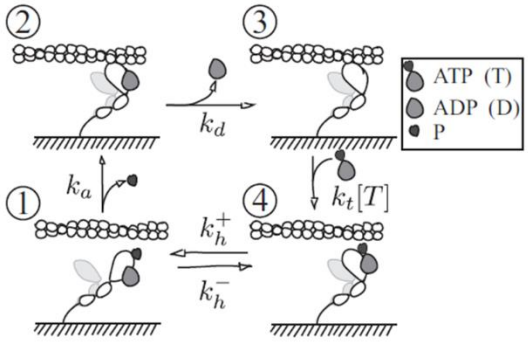

Figure 3.5. Cartoon of the 4-state kinetic model. Myosin transitions from a weakly bound state (1) to a strongly bound state (2). It then releases ADP, entering a rigor state (3). ATP binds to myosin, causing actomyosin dissociation (4).

model. This mathematical model incorporates a four-state kinetic model of the crossbridge cycle (figure 3.5), with global and local coupling. Here, global coupling refers to myosin molecules that affect each other's kinetics through the thin filament. For example, as a leading myosin pulls on the actin filament, a trailing myosin will feel this pull, release ADP and subsequently release actin. This load-sensitivity of myosin is well documented (47, 110, 121). Local coupling refers to myosin's ability to influence neighboring myosin and their ability to bind to the thin filament. The model employs a flexible chain model, where tropomyosin is treated as a flexible chain that can be distorted by myosin strong binding. The model depends on two key parameters: $\varepsilon(Ca^{++})$, the single myosin molecule transition from weak to strong binding as a function of Ca^{++} relative to the weak to strong transition rate in the absence of the regulatory proteins, and ℓ, the coupling distance, such that two myosin within this distance that are strongly bound to the thin filament completely activate the area of the filament between them, but act independently if they are separated by a distance greater than ℓ. The model has fit data from multiple scales, including single molecule, small ensemble, and motility data (28, 126-128). In previous work, this model has assigned ℓ to equal 400 nm. Note that this is not the same as the cooperative unit length, as ℓ only implies partial activation. For example, in this model, unattached myosin that are close to a strongly bound myosin are much more likely to bind than myosin that are farther away (but still within 400 nm). We assumed that this ℓ is independent of Ca^{++}.

The parameter ε is defined with the following equation:

$$\varepsilon = \varepsilon_{min}^{1-\theta} * \varepsilon_{max}^{\theta}$$

where θ is the fraction of Tn bound to Ca^{++}. This equation relates troponin's binding of Ca^{++} to myosin's ability to bind strongly to the thin filament. From previous work, we have estimated ε_{min} to be 0.006 and ε_{max} to be 0.5 (126). This equation is cleverly designed: if θ is near its maximum of 1, ε_{min} goes to 1 while ε_{max} goes to 0.5. Completing the equation results in $\varepsilon = 0.5$, suggesting that even in saturating Ca^{++}, myosin only binds half as well to regulated actin as it does to unregulated actin. Conversely, when Ca^{++} is low, ε_{min} goes to 0.006 while ε_{max} goes to 1, so that completing the equation would result in $\varepsilon = 0.006$. Thus, myosin's ability to bind to regulated actin can be mathematically modeled using the myosin binding rate to unregulated actin and θ, the fraction of Troponins bound with Ca^{++}.

We assume that Tn binding to Ca^{++} is fit by Michaelis-Menten and is determined by the equation:

$$\theta = \frac{[Ca^{++}]}{K + [Ca^{++}]}$$

Considering our assumptions, the only parameter that determines $\varepsilon(Ca^{++})$ is K, TnC's affinity to Ca^{++}.

***In Vitro* Motility Assay**

Background

In the *in vitro* motility assay, a nitrocellulose-coated coverslip is secured to a glass microscope slide, creating a 'flowcell'. Isolated myosin in solution is pipetted into the flowcell and adhered to the nitrocellulose. Fluorescent actin filaments are then flowed in, and the myosin on the surface can strongly bind to filaments (figure 3.6). When regulatory proteins are used, they are flowed in and allowed to incubate with the actin for seven minutes to ensure complete reconstitution of thin filaments (17, 57). Finally, the

motility buffer is added, with the appropriate pH and Ca^{++} conditions, as well as ATP to drive crossbridge cycling.

The fluorescent filaments are visualized as myosin propels them across the surface. The filament movement can be observed and recorded, and the velocities can be determined by measuring the distance traveled and the frame rate of the recording camera.

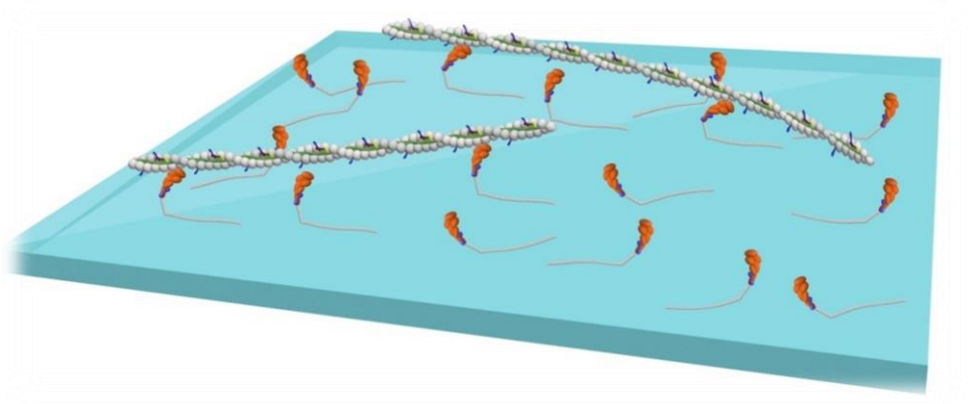

Figure 3.6. Cartoon of *in vitro* motility assay. Schematic of actin filaments (white) moving a surface of myosin molecules (orange). Figure courtesy of Mike Woodward.

The hardware and software, proteins, solutions, and assay are all similar to or encompassed by those of the laser trap assay. What follows is a brief description of the assay with key differences from the laser trap assay discussed.

Proteins

All proteins used in the motility assay are exactly the same as described above.

Solutions

Like the laser trap assay, myosin was ridded of dead heads and diluted, this time to 100 µg/mL for most experiments (the duty cycle requires a range from 5 to 100 µg/mL). The final buffer was the same as before except 1% methylcellulose was added, a crowding agent that keeps filaments near the myosin-coated surface, and 2 mM ATP. On

the day of the experiment, actin was diluted to 10 nM as before, but this time in the absence the regulatory proteins, which was incorporated directly in the flowcell. The day of the experiment, troponin and tropomyosin was diluted to 0.75 μM and 0.25 μM, respectively, and mixed in AB with additional KCl. Further, 100 nm excess troponin and tropomyosin was added to the motility buffer to ensure complete regulation of the thin filaments (17, 57). For the large ensemble experiments, both ATP and Ca^{++} were manipulated in the motility buffer. For the pCa-velocity experiments comparing wild-type and R146G troponin, the Ca^{++} was manipulated. For the ATP experiments, the ATP concentration was manipulated for both the wild-type and the R146G mutation.

In Vitro Motility Assay

As before, myosin was added to the flowcell followed by BSA, which was allowed to incubate for one minute. After one minute, vortexed unlabeled actin is flowed in, which is another preventative measure against any 'dead-head' myosin. All myosin will bind to the unlabeled actin, but after ATP is added 30 seconds later, the live myosin will dissociate from the unlabeled actin. Additional ATP was added to ensure all live myosin have released the unlabeled actin. Labeled actin was then added and allowed to bind to the myosin for one minute. Labeled actin was again added, and incubated for another minute. The regulatory proteins were then added and allowed to incubate with the labeled actin for at least seven minutes. Finally, the motility buffer with the appropriate level of Ca^{++} and ATP was added.

Hardware and Software

Labeled actin velocity was visualized with an ICCD camera (XR/MEGA-10EX™ S30, Stanford Photonics Inc. Palo Alto, CA). This camera is attached to a Nikon Eclipse

Ti® inverted microscope with a 100x, oil-coupled, 1.4NA objective. Video frames were acquired through an Epix-LVDS frame grabber (Epix, Inc., Buffalo Grove, IL) and controlled using Piper Control™ software (Stanford Photonics, Inc. Palo Alto, CA). TRITC filters (Thor Labs, Newton, NJ) are incorporated into the optical path to excite and visualize the filament on the ICCD camera. The flowcell was maintained at 30°C with an objective temperature controller (20/20 Technologies Inc. Wilmington, NC). For each flowcell, three videos of different fields were recorded to get a sufficient sample of filament velocity, at 10 frames per second for 30 seconds.

Regulated Thin Filament Velocity Analysis

Each video was analyzed using the ImageJ plugin WRMTRK, which skeletonizes each filament and determines distance traveled per unit time. This program tracks the filaments that fit the chosen parameters and output an average velocity for each field. Our parameters are as follows: to be considered moving, a filament must be at least 0.5 μm long and travel for at least three seconds.

Each experimental condition was performed at least three times. Each video typically captures 50-150 filaments. For the pCa-velocity measures, the data for each troponin variant was fit to the Hill equation to generate parameters (pCa_{50}, Hill coefficient) for inferential statistics. Goodness-of-fit was determined with the R^2 value. Significant differences in the Hill coefficient and the pCa_{50} were determined in a one-way ANOVA. For the duty cycle experiments, the data were fit to equation

$$V = V_{max} * (1 - (1 - f)^N)$$

where V is velocity, f is duty ratio, N is number of myosin heads (120). The major output, f, was statistically compared between the wild-type and R146G mutation by

comparing the value and the standard error to the fit. Similarly, the ATP experiments were fit to an exponential and the K_m was statistically compared between the wild-type and R146G mutation by comparing the value and the standard error.

CHAPTER 4

RESULTS

We characterized thin filament regulation on the molecular level by directly observing single molecule interactions between myosin and a regulated thin filament in a three-bead laser trap assay. This is the first time, to our knowledge, that single myosin binding has been detected with a regulated thin filament in the three-bead laser trap assay. With a single myosin, our main measure was frequency of binding, which increased as Ca^{++} levels were increased. We then observed a small ensemble of myosin interact with a regulated thin filament and measured force, duration, and the time between events. The measurement of force, duration, and binding frequency of a small ensemble of myosin interacting with a regulated thin filament is a novel achievement and is a key step in bridging the gap in our understanding of single myosin kinetics to single fiber and whole muscle actions. Again, our measures were a function of Ca^{++}, where force and duration increased and the time between events decreased as Ca^{++} was increased. Finally, we measured velocity as a function of Ca^{++} and ATP. In these experiments, high Ca^{++} produced velocities that follow a typical Michaelis-Menten relationship, while at low Ca^{++} there exists an ideal ATP level to initiate velocity and thus thin filament activation. In addition to our measures for thin filament activation, we tested the R146G Tn mutation in the *in vitro* motility assay. Our pCa-velocity results agree well with previous pCa-force and pCa-ATPase data, showing an increase in Ca^{++} sensitivity. We then teased out details of myosin's kinetics, where the mutant was shown to reduce myosin's duty cycle and reduce myosin's ADP release rate.

Effect of Ca^{++} on Single Myosin Binding

We first tested the effect of Ca^{++} on thin filament activation by measuring the rate of binding between a single myosin and a regulated thin filament in the three-bead laser trap assay. At pCa 4, the binding rate was 0.85 events per second, and this rate slightly increased to 1.11 at pCa 5, but then dropped to 0.45 at pCa 6 and then 0.23 at pCa 7 (table 1). Binding events were not detected at pCa 9, despite over 100 recordings totaling more than 9 minutes. Therefore, we have included a value for pCa 9 published previously for comparative purposes (62). These data are summarized in table 1. Sample traces show either many events (pCa 4) or very few events (pCa 7) depending on the Ca^{++} concentration (figure 4.1). The rates achieved at pCa 4 and 5 are about half of rates achieved with an unregulated thin filament (2.2 events per second), in agreement with other work that has examined single molecules interacting with a regulated thin filament (29).

In our experimental set up, placing the thin filament above the 3 μm mogul so that myosin can bind is crucial. If the filament is too high in the experimental chamber, myosin will not be able to reach the filament. To be sure that our low binding frequency at low Ca^{++} was not simply due to this experimental error, we measured the height of the actin filament under different Ca^{++} concentrations. This was done by taking an image of the 3 μm bead and using the airy disk to determine height. We found that the height across conditions was not significantly different (figure 4.2). We also found that the step size and attachment time of binding events were not significantly different across pCa levels (figure 4.3 and 4.4)

Effect of Ca^{++} on Binding of a Small Ensemble of Myosin

We then tested the effect of Ca^{++} on the ability of a small ensemble of myosin to bind to and generate force against a regulated thin filament in the three-bead laser trap assay. These experiments could shed light upon cooperativity in muscle, where one myosin's binding to actin increases the probability of a nearby myosin binding. Based on our myosin concentration and estimates of myosin availability, we suspect 6 to 8 myosin heads were available to bind to the regulated thin filament (27). Hundreds of events were recorded and plotted in a histogram (figure 4.5). At pCa 5, a wide distribution of forces was generated, from 0.2 to 10.8 pN, suggesting that an event can be composed of either a single head binding and releasing, multiple heads binding and then releasing, or multiple heads binding, cycling multiple times, and then releasing. As the Ca^{++} was reduced to pCa 6, 6.5, and 7 the peak forces decreased to 9.4, 5.0, and 2.8 pN, respectively. An analysis of the data using the non-parametric Kruskall-Wallis ANOVA followed by Dunn's post hoc tests found no significant difference between pCa 5 and pCa 6, but did see a difference between pCa 6 and pCa 6.5 as well as pCa 7. The comparisons are summarized in table 4.2. The duration of events also had a broad distribution and decreased with reduced Ca^{++} levels, coinciding with the force values (figure 4.6). Indeed, the relationship between force and event duration form a linear relationship (figure 4.7).

In addition to measuring force and duration of each event, we also measured the time between events (figure 4.8). This information provides insight into the strong binding of the first myosin molecule. We prefer the measure of time between events over binding frequency with the small ensemble data. This is because an "event" with small myosin ensembles can include many actomyosin interactions, especially those events that

produce large forces. Therefore, the time between events can provide insight into the rate of binding of the first myosin molecule at the start of any event, regardless of the event's peak force and duration. At pCa 5 the distribution of time between events was dominated by short times: approximately half of the time another event occurs within 100 ms. As the Ca^{++} is reduced, this percentage drops, and at pCa 7 often more than a second would pass before another event occurred. As the Ca^{++} was reduced to pCa 9, events became very infrequent, where the time between events was often 5 seconds or more. We were able to use the event duration data with the time between events data to calculate the percentage of time where at least one myosin head was strongly bound. At pCa 5, this value was 31%, but it decreased to 10% and 2% at pCa 6 and 7, respectively.

Effect of Ca^{++} and ATP on Binding of a Large Ensemble of Myosin

Finally, we performed the *in vitro* motility assay with regulated thin filaments and measured velocity as a function of Ca^{++} and ATP (figure 4.9). This method can provide insight into the importance and role of Ca^{++} and myosin in thin filament activation. At ATP levels <60 μM, the filaments were motile and the velocity was not different across pCa levels. The most logical explanation for velocity at low ATP is thin filament activation through myosin rigor binding. One myosin binding pushes the tropomyosin into open state, revealing additional myosin binding sites on actin nearby. The activation here is slightly different than that which occurs under physiological conditions because the ATP is low. Because the ATP concentration is low, the initial myosin binding event lasts a considerable amount of time, providing ample time for nearby myosin molecules to bind to the regulated thin filament. Thus, rigor activation occurs at an ATP concentration where heads are bound long enough to enable nearby myosins to bind, but

short enough to allow processive movement. As the ATP was increased, however, the velocities diverged in a Ca^{++} dependent manner. For example, at pCa 9, filaments ceased to move, but at pCa 4 the filaments approached maximum velocity. The peak velocity for each pCa level was widely distributed, with the largest difference between successive Ca^{++} concentrations existing between pCa 6.5 and pCa 7.

Mathematical Model

The mathematical model can be used to determine TnC's affinity for Ca^{++} in all three experiments (single molecule, small ensemble, large ensemble). We can also test the model to determine if a coupling distance of 400 nm is appropriate. The single molecule experiments don't have coupling, and therefore provide a clear picture of the role of Ca^{++} on myosin's weak to strong transition rate. The rates we observed were very low (~1 event per second) compared to the transition rate observed in solution (~40/s) (68, 94). This is most likely due to fluctuations in the thin filaments position relative the single myosin molecules and not an effect on the myosin's kinetics per se. When correcting for this, the data are well fit by our model (figure 4.10) (see equations in Methods: Mathematical Model), and generate a value for K of 0.216 ± 0.055 μM.

The small ensemble experiments have both Ca^{++} and myosin strong binding activation. Here, we can use the model to separate the effects of these two activators, as well as test the model's assumption of a local coupling distance of 400 nm. To do this, we simulated data to match the raw the data. The model was able to reasonably replicate the data (figure 4.11). We varied K to in the model to best replicate the raw data. This resulted in K = 0.199 ± 0.044 μM. This lines up well with our previous estimate of K = 0.216 ± 0.055 from the single molecule data.

To further test the model, we collected data with large ensembles with motility experiments. This leads to strong local coupling, as the concentration of myosin was 100 μg/mL. In such conditions, myosin can activate the thin filament through strong binding, even at low Ca^{++}. This is achieved by reducing the ATP levels and thus prolonging the strongly bound rigor state of myosin. Such conditions allow one strongly bound myosin to push tropomyosin, allowing neighboring myosin to strongly bind as well. In the absence of Ca^{++}, we found that rigor myosin were able to activate the thin filament and increase velocity as a function of ATP. We found that for low Ca^{++} conditions (pCa 9), 60 μM ATP was a critical point, where velocity decreased as ATP was increased beyond 60 μM. This agrees well with previous data (62). We tested the role of strong binding activation by repeating these experiments with different Ca^{++} concentrations. We found that 60 μM was a critical point for many other Ca^{++} concentrations. We used the model to match the experimental data (figure 4.12). We determined values of ε to optimize the fit of the data. The data were well fit by equations (1) and (2), and generated a value for K = 0.217 ± 0.034 μM.

The estimate of ε along with the fits are surprisingly similar to the fits generated for the single molecule and small ensemble data. The model is able to explain thin filament activation across many levels, and is able to tease apart the role of Ca^{++} and myosin strong binding on thin filament activation.

R146G Mutation

In addition to examining thin filament activation with wild type regulatory proteins, we examined the effect of a cardiomyopathy-inducing mutated troponin. This particular mutation has proven to be a difficult to understand due to the lack of consensus

of the mutation's effect as well as the odd result that the mutation seems to not only affect myosin's on-rate but also other steps of the crossbridge cycle (we expect troponin to affect myosin's weak to strong transition, but not other steps such as ADP release or ATP binding). To address this, we measured the velocity of regulated thin filaments in the *in vitro* motility assay either in the presence or absence of the mutant.

The Effect of the R146G Mutation on pCa-Velocity

Our first test was to examine the mutant's effect on the pCa-velocity relationship (figure 4.13). Under high Ca^{++} concentrations, the filaments with the R146G mutation are moving but are significantly slower than filaments with wild-type troponin. However, under low Ca^{++} conditions, filaments with the mutation move significantly faster than wild-type. Similar findings have been found with force measurements in muscle fibers (69, 70, 114, 129). The reduced velocity under high Ca^{++} conditions and the relative increase in velocity under low Ca^{++} conditions may explain the data's poor fit to the Hill equation. The wild type is well fit with the Hill equation ($R^2 = 0.97$), however, the mutant is poorly fit ($R^2 = 0.31$). The results also show a leftward shift in the curve and a subsequent increase in the pCa_{50}, suggesting earlier activation with the mutation. This result is in agreement with many (12, 34, 70, 114, 129), but not all (69), of the previous studies examining this mutation's effect on Ca^{++} sensitivity in force and ATPase measurements.

The Effect of the R146 Mutation on duty cycle

To identify the mechanism of the R146G mutation, we measured the velocity of thin filaments in a duty cycle motility assay. In this motility assay, the myosin concentration is manipulated and the resulting velocities are fit to the duty cycle equation

(see Methods: Regulated Thin Filament Velocity Analysis*)* (120). This assay gives an estimate of the percentage of myosin heads bound to the regulated thin filament at any given moment. The increase in the pCa_{50} suggest that the mutant would increase the duty cycle, however, our results show a slight decrease in duty cycle in the presence of the mutation, from 1.81% to 1.39% (figure 4.14). Our results also showed a reduced velocity, even at maximum myosin concentration, from 4.63 ± 0.15 μm/s with the wild-type to 2.49 ± 0.11 μm/s with the mutant. To be sure that this didn't affect our duty cycle result, we normalized the duty cycle results; this however, did not change the outcome. A possible explanation for the pCa-velocity and duty cycle results is that the R146 mutant slows ADP release, leading to slower maximal velocities but higher velocity at low Ca^{++}, in addition to dramatically reducing myosin's on-rate. If the on-rate is slowed significantly more than the ADP release rate, the overall effect would be a reduction in the duty cycle, as we observed.

The effect of the R146G Mutation on ADP release

To further explore the effect of the mutant on myosin's kinetics, we measured regulated thin filament velocity as a function of ATP concertation (figure 4.16). These data were fit to a Michaelis-Menten relationship and the parameters are shown in Table 4.3. Again, the maximum velocity was reduced in the presence of mutation relative to the wild type, decreasing from 4.54 ± 0.13 μm/s to 2.56 ± 0.06 μm/s. To examine ADP release rate, the data was converted to time on (t_{on}), which is the displacement generated by 1 myosin head, assumed to be 10 nm (d=10 nm), divided by the velocity of the thin filament ($t_{on} = d / V$). The t_{on} data can then be used to estimate ADP lifetime and rigor lifetime, assuming that t_{on} is made up entirely of ADP lifetime at saturating ATP and that

t_{on} = the time of the ADP lifetime plus the time of rigor where myosin is waiting for ATP to induce actomyosin dissociation ($t_{on} = t_{\text{-ADP}} + t_{rigor}$). Our results show a reduction in the ADP release rate in the presence of the mutation (figure 4.17, table 4.3), decreasing from 401.3 s^{-1} with the wild type to 248.4 s^{-1} with the mutant.

CHAPTER 5

DISCUSSION

With our first set of experiments, we were able to examine thin filament activation and tease apart the role of Ca^{++} and myosin strong binding. Our first set of experiments give us a better understanding of thin filament activation under normal conditions, and we hope to use this knowledge to examine perturbations, such as acute changes in metabolites or chronic mutations in key muscle proteins. In our second set of experiments, we examined a specific mutation in troponin that is associated with cardiomyopathy.

Thin Filament Activation

According to the 3-state model (81), thin filament activation requires both Ca^{++} binding to Tn as well as myosin strong binding to the thin filament. However, the role that each of these play in activation are unclear. Some have suggested that strong binding doesn't play a crucial role under physiological ATP levels (41). Others have suggested that myosin's weak to strong binding transition is Ca^{++} independent (16). To better understand the significance of each mechanism, we directly observed single molecules, small ensembles, and large ensembles of myosin bind to actin under a spectrum of Ca^{++} concentrations. This is the first time, to our knowledge, that force and motion of single and small ensembles of myosin have been directly observed under such a wide range of Ca^{++} concentrations. Such experiments give us a bottom-up view of thin filament activation and can help us tease apart the role of Ca^{++} and strong myosin binding.

Single Molecule Binding

Single myosin binding to a single thin filament was observed in the laser trap at various Ca^{++} levels. As Ca^{++} is reduced, binding events became less frequent, declining from 0.85/s at pCa 4 down to 0.02/s at pCa 9. This data agrees with models that suggest Ca^{++} affects myosin's weak to strong binding transition and disagrees with models that suggest Ca^{++} alters other kinetic steps, such as phosphate release (16). Our data and model do also do not support the notion that Ca^{++} has an allosteric effect on the thin filament which controls myosin binding (16, 53, 117).

Even at saturating Ca^{++}, the binding frequency was only 0.85/s, more than half the binding frequency observed with an unregulated actin filament (2.2/s). Similar findings have been obtained in a landing assay, where the ability of S1 myosin to land on a Ca^{++}-activated thin filament was reduced compared to an unregulated actin filament (29). Mathematical models have included this, suggesting that there is still an energy barrier that myosin must overcome, even at saturating Ca^{++} (126, 127). Solution experiments have also shown that ATPase is inhibited at low S1 myosin concentrations in the presence of regulatory proteins and saturating Ca^{++} (72).

Under the conditions of the laser trap, the thin filament is placed close to the top of the 3 μm myosin-coated mogul. In this experiment, the height is crucial: filament heights above 3.5 μm or below 3.0 will result in either no binding or unproductive binding between either actin and myosin or actin and the surface of the mogul. Differences in height across Ca^{++} concentrations could lead confounding results. To ensure our single molecule binding was indeed Ca^{++} dependent and not due to experimental error in height, an image of the mogul was captured during data collection and analyzed after the experiment. Any recordings collected out of our range of 3.0 to 3.5

μm was disregarded. We found that the height of the thin filament was not significantly different from pCa 4 to pCa 9 (figure 4.2)

Myosin Ensembles

Our single molecule binding frequency data could be fit to a pCa curve. Though the fit is good (figure 4.10), the Hill coefficient is low (1.4 ± 0.3)This does not agree well with pCa-force curves, which can show Hill coefficients up to 6 (9). Our low Hill coefficient confirms that some cooperativity exists even in the absence of multiple myosin. Cooperativity can occur in four main ways: 1) coupling between the two Ca^{++} binding sites on fast skeletal TnC, 2) coupling between Ca^{++} binding sites down the thin filament, 3) myosin strong binding inducing Ca^{++} binding to TnC, and 4) myosin strong binding inducing movement of tropomyosin into an open state so other myosin can more easily bind (44). The first two mechanisms may play a role, but can only produce Hill coefficients up to 1.2 or 1.5, respectively (46). Though these mechanisms contribute, they do not seem to be the main mechanism(s) of the cooperativity observed in thin filament activation. Mechanism (4), where myosin strong binding induces other neighboring myosins to strongly bind, could play a larger role than other mechanisms. Indeed, the importance of strong myosin binding has been demonstrated with NEM myosin, which strongly bind to actin but do not release. Experiments have shown that rigor or NEM myosin are capable of activating a thin filament (49, 111). Experiments with fluorescent probes in fibers (112) have compared the overlap region to the nonoverlap region and showed that endogenous myosin binding leads to S1 binding in the overlap region, but not in the nonoverlap region. Though many examples exist to demonstrate strong-binding cooperativity, some question the physiological relevance of this mechanism (41). This

concern is valid, as these previous experiments were done at very low ATP, much lower than physiological levels. Recent work has shown that Tn and Tm dynamics are much faster than myosin kinetics, suggesting that myosin strong binding would not play a large role in activation (41).

By using a small ensemble of myosin in the laser trap at 100 μM ATP, we could examine the role of myosin strong binding under near-physiological conditions. This ATP concentration is up to 1,000x typical myosin strong binding experiments. Further, with this ATP concentration, we would expect short but detectable (10 ms) binding durations per each myosin. At high Ca^{++}, the myosin ensembles produced a wide distribution of forces. Interestingly, most of the events produces low force (1-2 pN), though some binding events went as high as 11 pN. As Ca^{++} was reduced, these larger forces disappeared. For example, the highest force produced at pCa 7 was 3 pN, and pCa 9 produced events that looked like single molecule events.

To further examine the role of Ca^{++} and strong binding myosin in activating the thin filament, we performed motility experiments while manipulating Ca^{++} and ATP. Previous work has shown that at high Ca^{++}, motility velocities are well described by a Michaelis-Menten relationship as ATP is increased. However, at low Ca^{++}, velocity rises up until ~60 μM ATP, and then slowly declines (62). We build off of this previous work by examining the effect of a wide range of Ca^{++} levels, from pCa 9 to pCa 4. Our data confirm that 60 μM is a critical ATP concentration.

Mathematical Model

To separate the effects of Ca^{++} and myosin strong binding, we compared our data to a mathematical model. The model was able to replicate the experimental data well at

all levels (single molecule, small ensemble, large ensemble). Impressively, the model generated values for the Tn- Ca^{++} binding affinity that are extremely similar across all three levels. In addition, the model was able to tease apart the role of Ca^{++} and myosin strong binding. Using the model, we were able to extrapolate force generation as if each myosin molecule acted independently (i.e., no myosin strong binding activation or cooperativity. The resulting pCa-force curve had a low Hill coefficient (1.4 ± 0.3) and low pCa_{50} value (5.96). Even if we tried to shift the curve to line up with pCa-force data collected in fibers, the curve is still not steep enough to match these data. However, once myosin strong binding activation is added into the model, the model is able to recapitulate a typical pCa-force curve. The model recapitulates data generated from single muscle fibers (85), with a Hill efficient of 1.7 ± 0.2 and a pCa_{50} of 6.81 (figure 5.1). Therefore, myosin strong binding activation is necessary to describe experimental data.

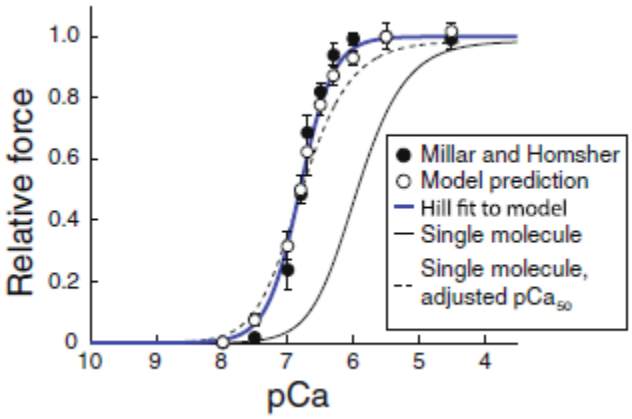

Figure 5.1. pCa-force relationship for single molecule data and our model. We fit our single molecule binding data to a pCa curve. This curve is shallow and shifted to the right compared to pCa-force data from fibers. The model incorporates cooperativity, and can therefore duplicate experimental data with an appropriate Hill coefficient and pCa_{50}.

The model predicts myosin are locally coupled if they are within 400 nm of each other. In the model, if two strongly bound myosin are within this range, then the thin filament is activated between the two myosins. Further, if one myosin is strongly bound, the probability of a neighboring myosin also binding is increased. This probability is affected by how close the second myosin is: the closer the second myosin is to the first

myosin, the higher the increase in probability of the second myosin binding. An important note is that this length of 400 nm (ℓ) is not the same as the cooperative unit length (μ), as ℓ implies only partial activation. In other words, an increase in the attachment rate would be miniscule 400 nm from the point of first attachment because the function drops off rapidly away from the site of first attachment. Assuming tropomyosin is a flexible chain, we feel that ℓ better captures the effect of strongly bound myosin, and the model better encapsulates myosin strong binding activation compared to models that use the cooperative unit. Further, the cooperative unit length has been hard to determine, with ranges from 40 nm to 500 nm (62, 74, 77, 80, 97, 103, 122). Meanwhile, ℓ has been determined to be 400 nm. Indeed, previous experiments have led to this conclusion (127), and our current results support this distance. In fact, for the model to fit our data, a coupling length of 400 ± 100 nm was not only sufficient but necessary. Thus, our data confirm the model's prediction of the coupling length between myosin, regardless of the number of myosin present.

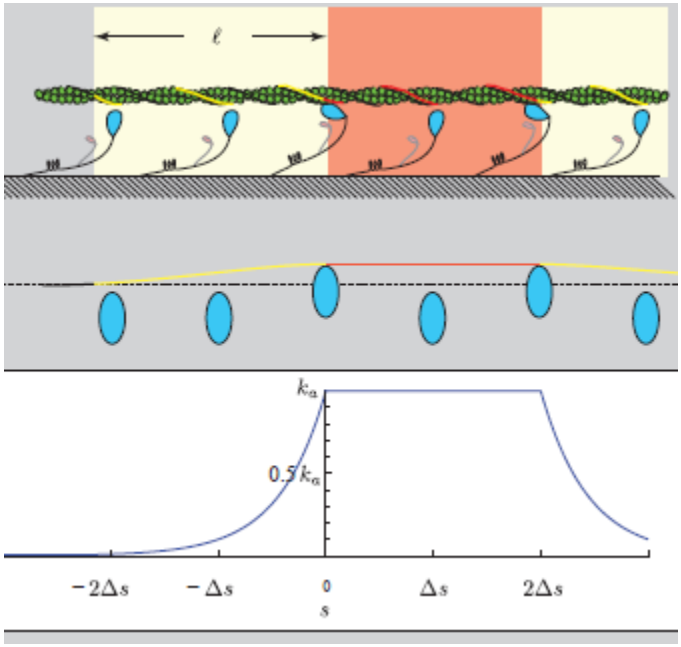

Figure 5.2. Depiction of the mathematical model. Top: two myosin activate the region between them (red). Regions with only one myosin bound (white) lead to partial activation for a distance. Middle: model of tropomyosin's position, depending on myosin strong binding. Bottom: probability (ka) of neighboring myosin binding.

Based on the myosin concentration used and the geometry of the experimental setup (in particular, the use of a 3 μm bead as a pedestal for myosin), we expect ~7

myosin molecules could interact with the thin filament (27, 51). The mathematical model we used suggests that 14-22 myosin were available. We attempted to reconcile this difference by using TIRF to quantify the number of myosin in a given area, and compare this value to the area on the 3 μm pedestal that would provide myosin the ability to bind to thin filament. Unfortunately, there was much variability in this experiment. Regardless of the exact number of myosin, the myosin molecules would have had to at least communicate over a distance of 36 nm. This assumes that the 3 μm pedestal bead provides a ~500 nm region where myosin can reach the thin filament. If 14 myosin were evenly spaced out on this 500 nm region, they would be 36 nm apart, on average. If the number of myosin was closer to 7, they would be 71 nm apart, on average. Thus, cooperativity observed in our experiments is likely not due to cooperative binding of myosin within a regulatory unit, but rather due to cooperative binding of myosin beyond their own regulatory unit. This concept is confirmed by our data, as the local coupling length in the model is 400 nm.

Limitations

The performed experiments do not go without limitations. Future experiments can provide more detail into the molecular mechanisms of thin filament activation with improvements on the current experiments. The first limitation is the use of 100 μM ATP. We chose this concentration because it allows us to detect many binding events. Higher concentrations could lead to events that occur so quickly that our system would not detect it (>5 ms). On the other hand, we wanted to ensure that myosin was in the form of ADP.P_i, and not ADP or rigor. We are confident, based on the ATP binding constant of myosin, that we achieved our goal.

The second limitation is the random configuration of myosin on the 3 μm mogul. To better recapitulate muscle *in vivo*, future experiments could use reconstituted thick filaments. Such filaments can be designed to not only duplicate the spacing of myosin *in vivo*, but could also be manipulated to add extra myosin or take myosin away. A nice feature would be the ability to count the myosin interacting with the actin filament. This could be done possibly by dual color microscopy, where the actin and myosin are labeled with different color fluorophores.

The third limitation is the shape of the 3 μm mogul. The curved surface of the 3 μm mogul leads to particular phenomena, such as different binding rates of the first and second myosin during a small ensemble run. Future experiments could examine a flat pedestal instead of round one. Maybe even more important is the ability to control the thin filament in the Z-axis. Current microscopes provide feedback to maintain the height of the experimental set up, but many do not have nm resolution.

R146G Mutation

Of the three subunits of troponin, the inhibitory region, TnI, is responsible for binding to actin in the absence of Ca^{++} and subsequently keeping tropomyosin in the blocked state. Upon Ca^{++} binding, TnI detaches from actin and binds to TnC, allowing tropomyosin to move freely over the actin surface. A key part of TnI's function is the inhibitory region, which spans residues 96-116 on skeletal TnI and 126-146 on cardiac TnI, and is responsible for binding to actin in the absence of Ca^{++}. This places our mutation of interest, R146G, just within this key inhibitory region.

The data for this mutant are equivocal for many measurements. Some have found that force is reduced in the presence of the mutant at maximal Ca^{++} (70, 129), but others

have not seen this (114, 132). Similarly, some have found that ATPase is reduced (70, 114), but others have not seen this (34, 129), and some have seen that velocity is reduced in motility (12), but not in fibers (60). The results make it difficult to say clearly if this mutant has an effect at all on peak force, ATPase, or velocity. However, most work agrees that there is a shift in the pCa_{50} across ATPase, force, and velocity measures (12, 60, 70, 114, 129, 132).

We have collected data in agreement with previous findings. Under maximal Ca^{++} conditions, we see a ~46% reduction in velocity. We also see a leftward shift in the pCa-velocity relationship. To try to tease apart the mechanism behind this, we examined the ADP release rate and the duty ratio. We found that the duty ratio decreased ~22%, from 1.8 to 1.4%. In separate experiments, we found that the ADP release rate was reduced by ~38%. What follows is set of possible explanation for these phenomena.

The observed decrease in velocity, even in the presence of maximal Ca^{++}, is in agreement with previous findings. The reduced velocity can happen if myosin's kinetics are altered. One of myosin's kinetic steps that may be slowed is the weak to strong transition. This is the step that the regulatory proteins control, and the R146G mutant may impede myosin's weak to strong transition more than the wild-type Tn. Previous data (29, 126, 127) and our data presented here suggest that the weak to strong transition rate is reduced in the presence of regulatory proteins, even at maximal Ca^{++}. The mutant may exacerbate this reduction. The structural mechanism could be that the mutant TnI, rather than binding to TnC at maximal Ca^{++}, stays attached to actin, keeping tropomyosin in the blocked state. Some of the TnI molecules may come off of actin, but a high enough percentage may stay bound to actin, preventing complete thin filament activation. To test

whether the myosin's weak to strong transition was limited, we performed duty cycle experiments. In these experiments, velocity is measured as a function of myosin concentration. The data can be fit to the duty cycle equation to determine the percentage of myosin molecules bound at any given time. The presence of the mutant induced a reduction in the duty cycle from 1.8 to 1.4%. These duty cycles are relatively low compared to previous measures, but a relative comparison would imply that myosin spend less time on actin in the presence of the mutant. This could be due to a reduction in the weak to strong transition rate.

Alternatively, the reduction in velocity could be due to a reduced ADP release rate. Our duty cycle experiments would suggest that this step is not the culprit, as a reduced ADP release rate would prolong myosin's time attached to actin and thus increase the duty ratio. This would be in disagreement with our findings. To be sure, we completed experiments to calculate the ADP release rate by measuring velocity as a funciton of ATP. We assume that the mutant does not affect the ATP binding constant of rigor myosin. When we fit these velocity-ATP data, we found that the ADP release rate was indeed reduced in the presence of the mutant. Based on the duty cycle experiments, the reduction in ADP release rate was not expected but is still possible: both the weak to strong transition rate and the ADP release rate may be slowed, but the former is slowed to a greater extent than the latter. This would lead to reduced velocity as well as a reduced duty cycle.

How the weak to strong transition could be altered by a Tn mutant may be easy to explain, how the Tn mutant would alter ADP release is unclear. The Tn mutant may interact with myosin and can alter its kinetics. Though this is possible based on the

proximity of myosin to the regulatory proteins, this Tn-myosin interaction seems unlikely, considering TnI can only reach two of the seven actin monomers in a regulatory unit, and would thus only be able to affect myosin if the myosin was bound to those actin monomers. Recent investigations have made progress in examining the interactions of myosin-thin filament residues using cryo-EM (124, 125), but currently lack the ability to characterize the loose C-terminal of TnI.

To further complicate matters, we found, in agreement with previous work, that the mutant induces a leftward shift in the pCa-velocity relationship. This would seem to complicate the story, as a leftward shift isn't expected when myosin's on-rate is slowed. However, a reduced ADP release rate may contribute to strong binding activation. The longer myosin stays bound to actin, the higher the probability of a neighboring myosin binding as well.

The pCa-velocity relationship in the presence of the mutant is not fit well (R=.307). Indeed, the difference in velocity between low Ca^{++} and high Ca^{++} is only 1 μm/s. It seems that the mutant isn't very sensitive to Ca^{++} at all. Others have shown that peak velocity or ATPase is reduced at maximal Ca^{++} compared to wild type, yet the thin filaments with the mutant are not able to completely inhibit ATPase activity. Assuming a three-state model of regulation, the vast majority (~99%) of myosin binding sites on actin should be blocked. However, the R146G mutation may limit TnI's ability to bind to actin, allowing tropomyosin to move freely around the closed state and increasing myosin's probability of binding to actin. Conversely, the mutated TnI may not bind to TnC as well as the wild-type during maximal Ca^{++} activation. Thus, thin filaments in the presence of the R146G mutation fluctuate between blocked, closed and open, regardless of Ca^{++}, and

the distribution of these three states is not strongly dependent on Ca^{++} compared to wild-type proteins. Others have confirmed this idea, suggesting that the R146G mutant stabilizes the closed position (61). Determining the precise distribution of open, closed, and blocked from our data is not possible, but future work examining single molecule and small ensembles in the laser trap, along with mathematical modeling, could provide insight.

Future work could examine how this mutant (and other mutants) affect single myosin molecule binding as well as other kinetic steps. This can be done using the laser trap assay. Our current findings suggest that both the weak to strong transition as well as ADP release are slowed in the presence of R146G. A single molecule laser trap assay would be able to directly observe this behavior. It would then be possible to examine how this single molecule behavior affects a small ensemble of myosin in producing force and motion. Further, these measures can be examined over a range of Ca^{++} concentrations, which would provide insight into the leftward shift in the pCa-velocity relationship.

TABLES AND FIGURES

Table 4.1: Events per Second for Single Molecule Binding Events

pCa	Events per Second
4	0.85
5	1.11
6	0.45
7	0.23
*9**	*0.01*

*pCa 9 was published by Kad 2005 (62)

Table 4.2: Significant Differences of Ensemble Forces between Ca++ Concentration

Comparison			Significant Difference
pCa 5	vs.	pCa 6	No
pCa 5	vs.	pCa 6.5	Yes
pCa 5	vs.	pCa 7	Yes
pCa 6	vs.	pCa 6.5	Yes
pCa 6	vs.	pCa 7	Yes
pCa 6.5	vs.	pCa 7	Yes

Table 4.3: Fit parameters for R146G data

Measure	WT	R146G
Vmax (μm/s)	4.54 ± 0.13	2.56 ± 0.06*
Km (μM)	264 ± 33	132 ± 17
ADP Lifetime (s)	0.0024	0.0040*
ADP Release Rate (s-1)	410.29	248.37*

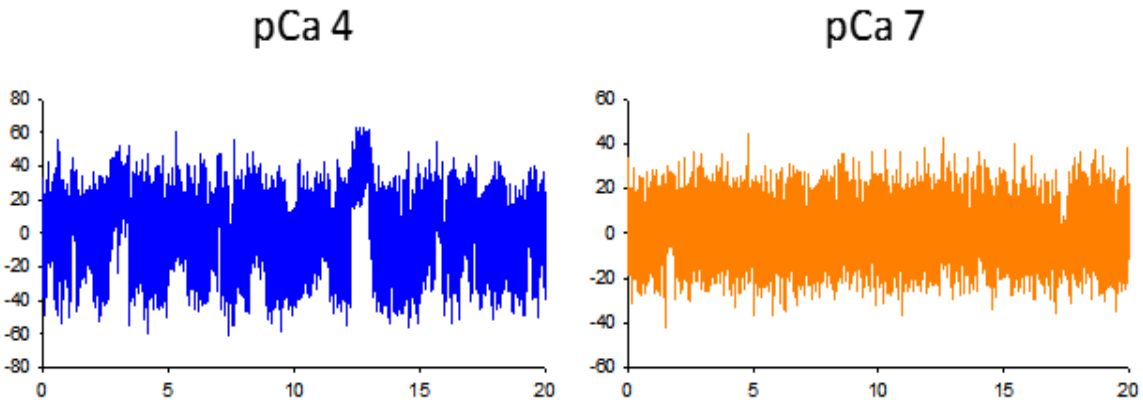

Figure 4.1. Sample traces of single molecule binding events at pCa 4 (left) and pCa 7 (right). Single molecule binding events became less frequent as Ca++ was reduced.

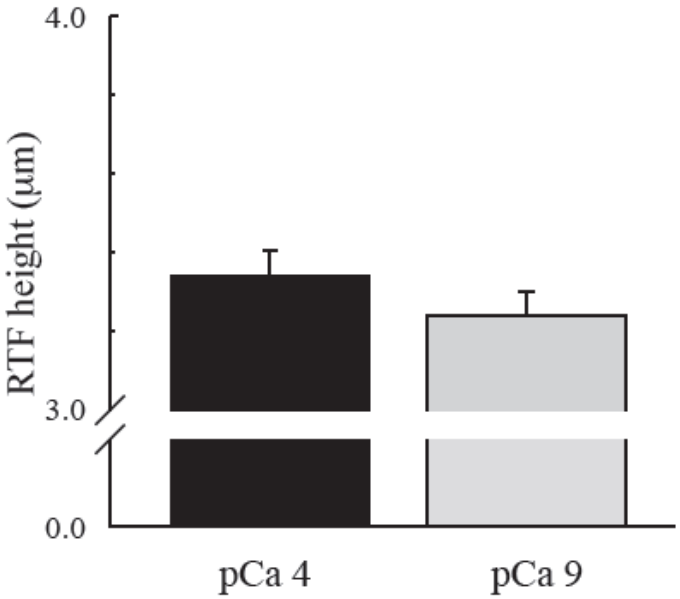

Figure 4.2. Height of a regulated thin filament in the single molecule laser trap assay. The height of the RTF was not significantly different from pCa 4 to pCa 9.

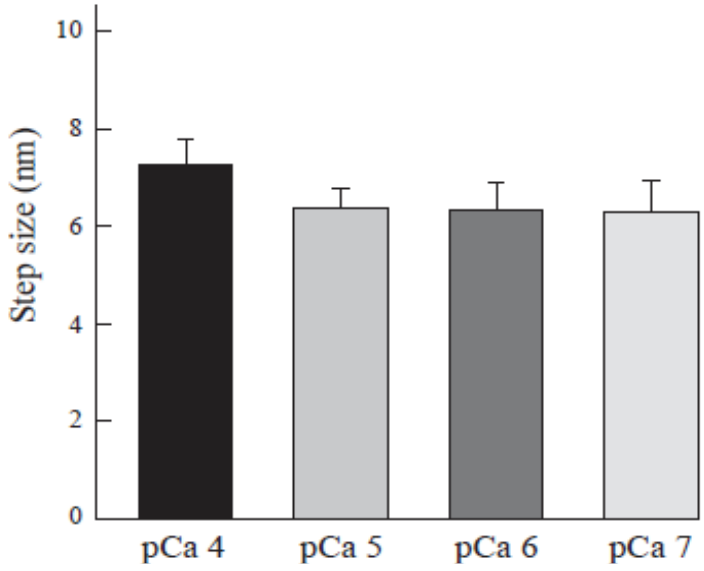

Figure 4.3. Step size in single molecule experiments. The step size was not significantly different across pCa levels.

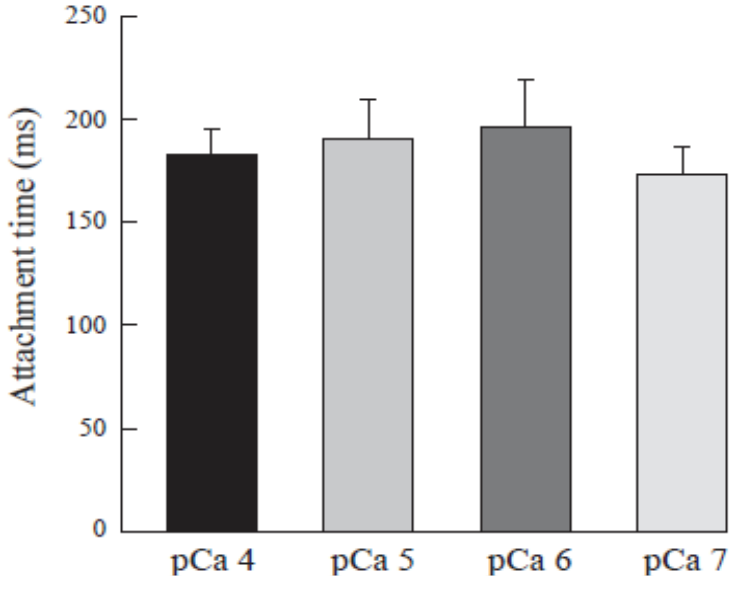

Figure 4.4. Attachment time during single molecule experiments. The attachment time was not significantly different across pCa levels.

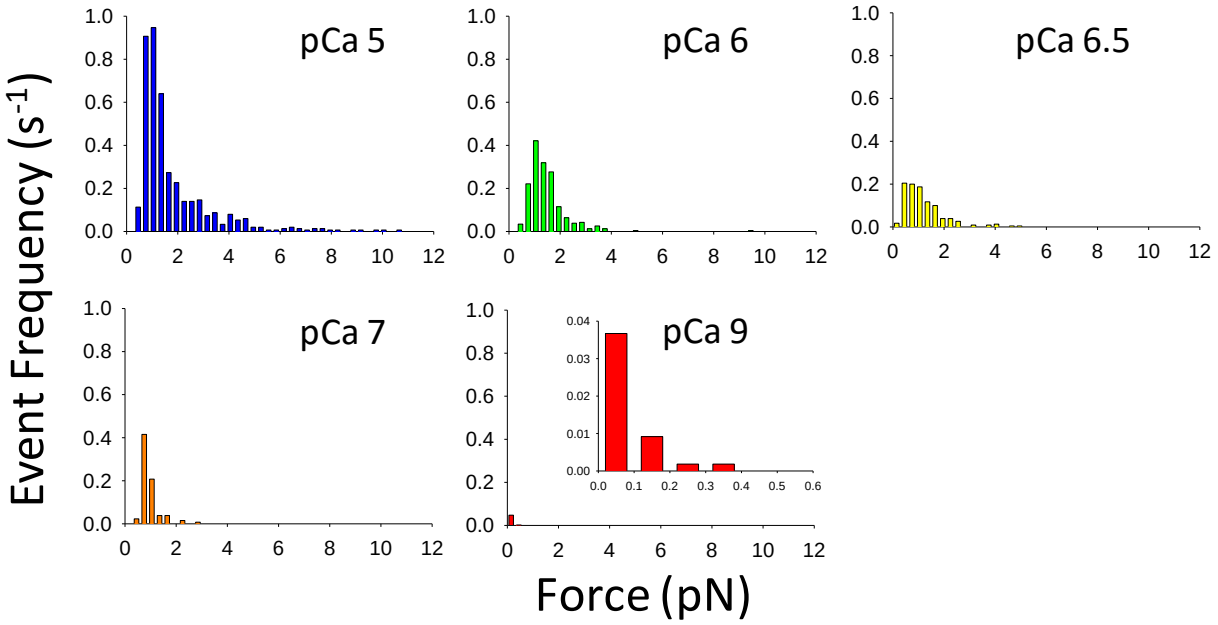

Figure 4.5. Force Histograms for each pCa. Events were most frequent and most likely to produce high forces at pCa 5. Event frequency and peak force declined as Ca++ was reduced. Events were extremely rare at pCa 9, as shown by the inset.

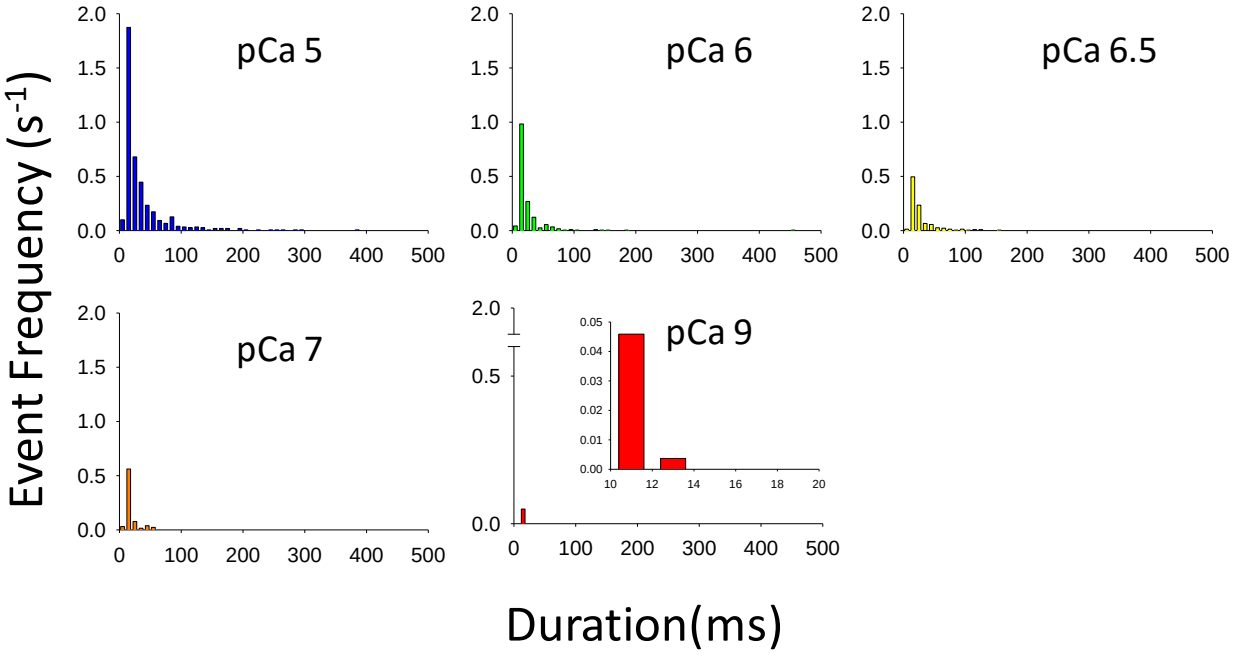

Figure 4.6. Histogram of Event Duration for each pCa. At pCa 5, events lasted for hundreds of milliseconds, but duration declined as Ca++ was reduced. Despite the high myosin concentration, events at pCa 9 typically lasted less than 15 ms.

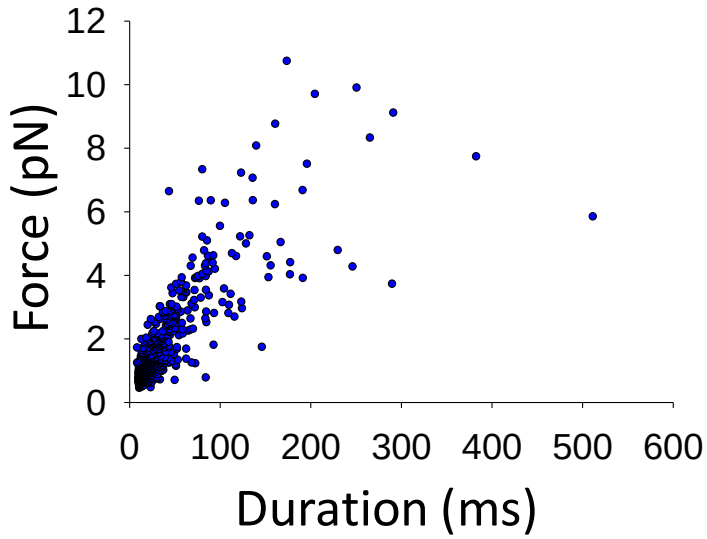

Figure 4.7. Relationship between Force and Duration at pCa5. As the myosin ensemble generated force, the event duration was prolonged.

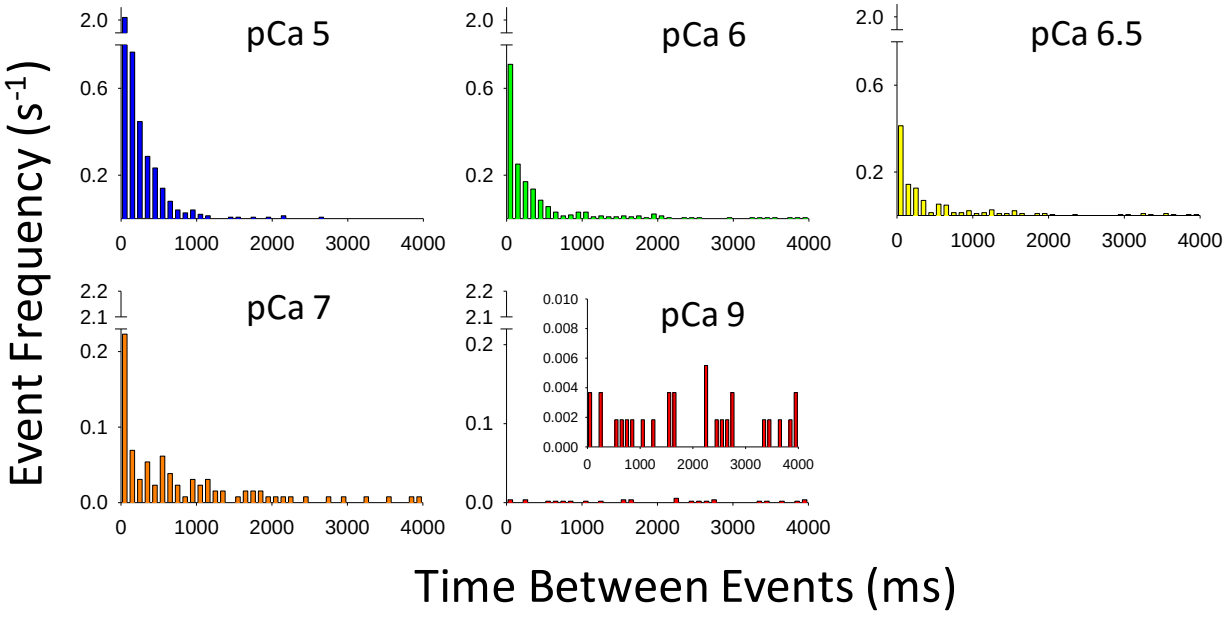

Figure 4.8. Time between events at each pCa. At pCa 5, events occurred in repid succession. However, as Ca++ was reduced, events became less frequent. At pCa 9, the time between events was many seconds.

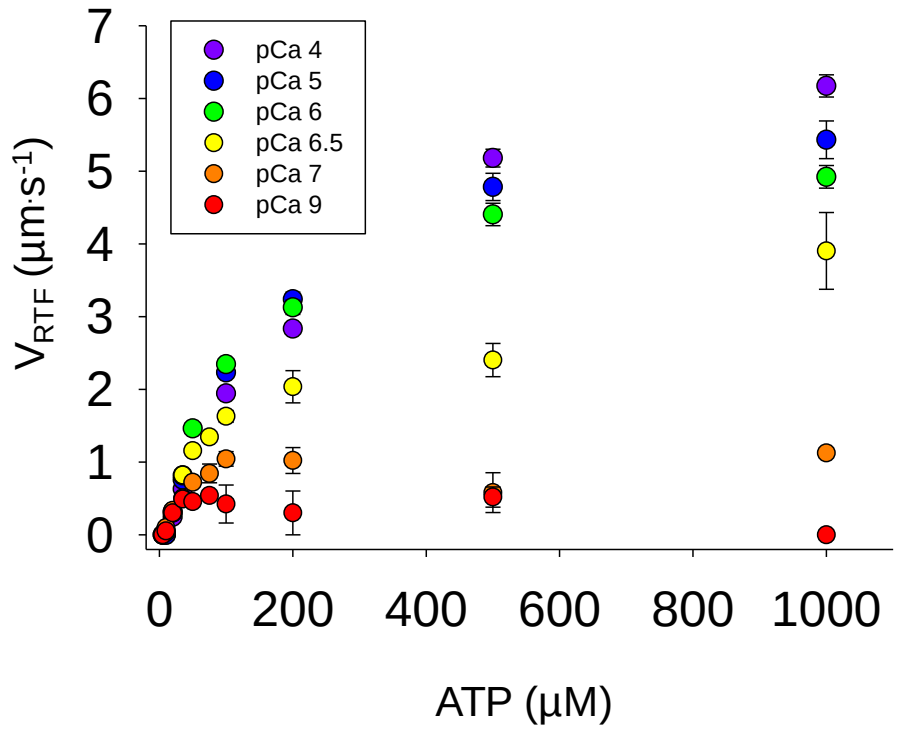

Figure 4.9. Velocity of regulated thin filaments as a function of Ca++ and ATP in an in vitro motility assay. At pCa 4, velocity follows a typical Michaelis Menten relationship. However, at pCa 9, there exists an ideal ATP level to generate maximum velocity. The velocity depends not only on actomyosin binding sites availability, which is partially dictated by Ca++, and myosin on-time, which is dictated by ATP binding.

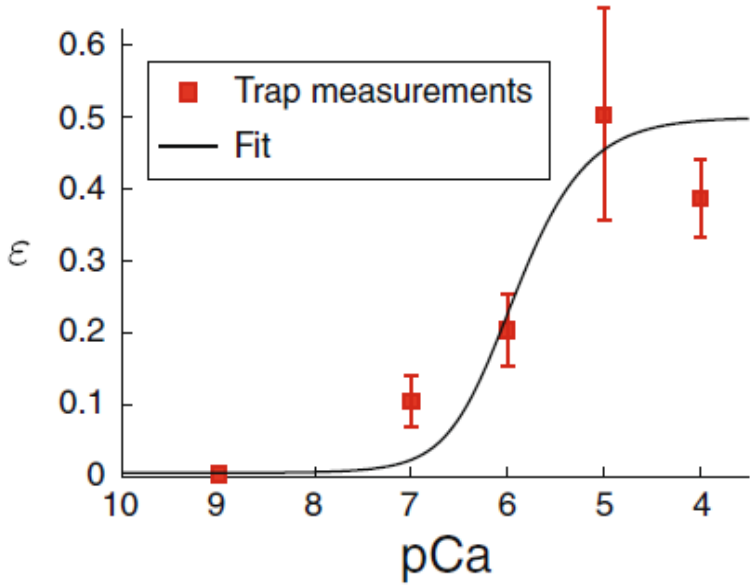

Figure 4.10. Comparing our single molecule data to the mathematical model. The single molecule binding rate directly measured was well fit by the mathematical model.

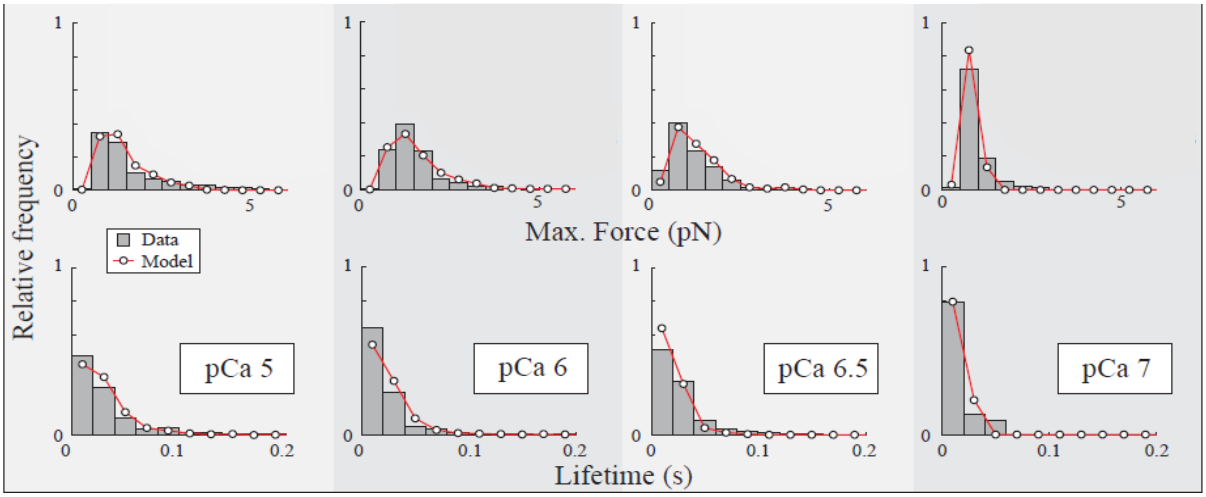

Figure 4.11. Comparing our small ensemble data to the model. The force and on-time were converted to a relative frequency (gray bars) and are well fit by the mathematical model (red line).

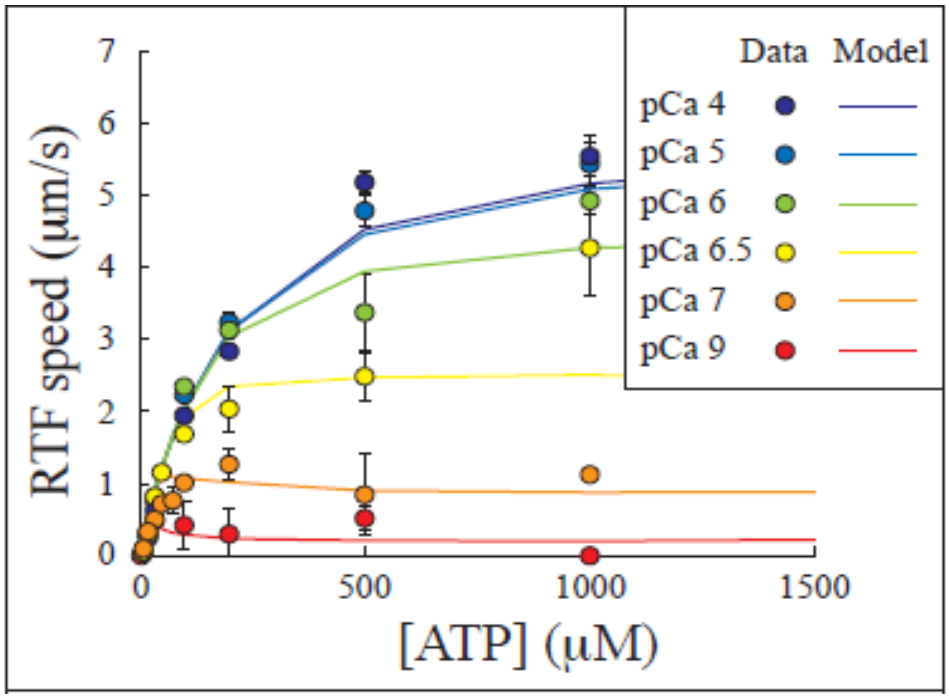

Figure 4.12. Comparing our large ensemble data to the model. The thin filament speed is well fit by the model, regardless of ATP and Ca^{++}.

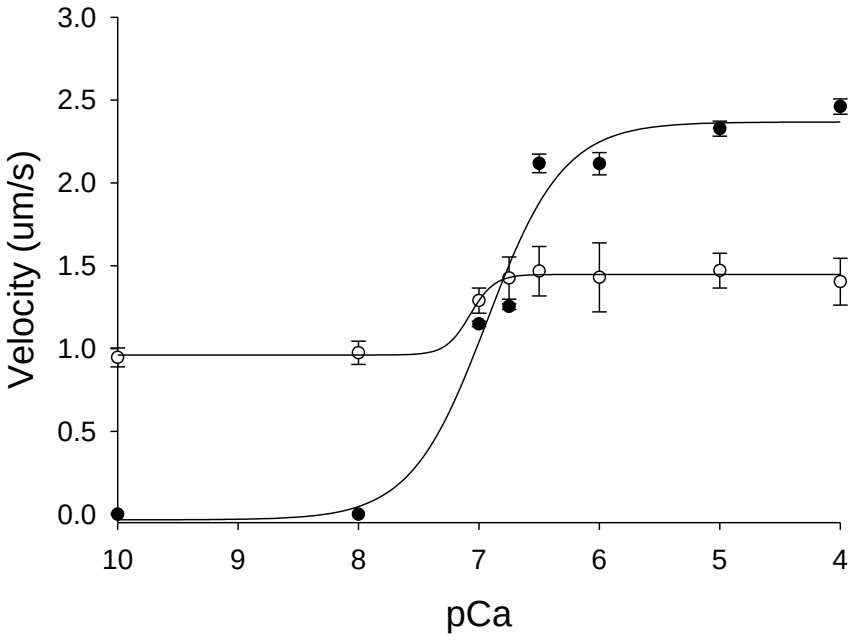

Figure 4.13. pCa-Velocity relationship generated in an in vitro motility assay. Wild-type (black) produced a typical sigmoidal curve, while the mutant (white) was poorly fit to the Hill equation due to low velocity at maximum Ca++ and elevated velocity at low Ca++.

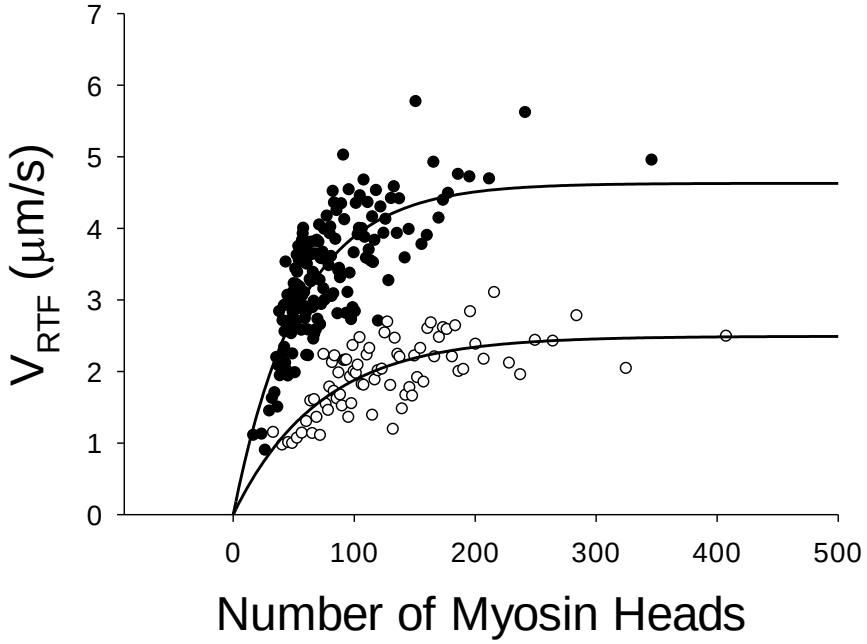

Figure 4.14. Velocity as a function of available myosin heads in an in vitro motility assay. Also known as a duty cycle assay, the myosin concentration was manipulated and number of heads available was estimated using the data in Harris and Warshaw 1993 (51). The duty cycle was slightly lower with the mutant (1.39%, white) while the wild-type (black) was 1.81%.

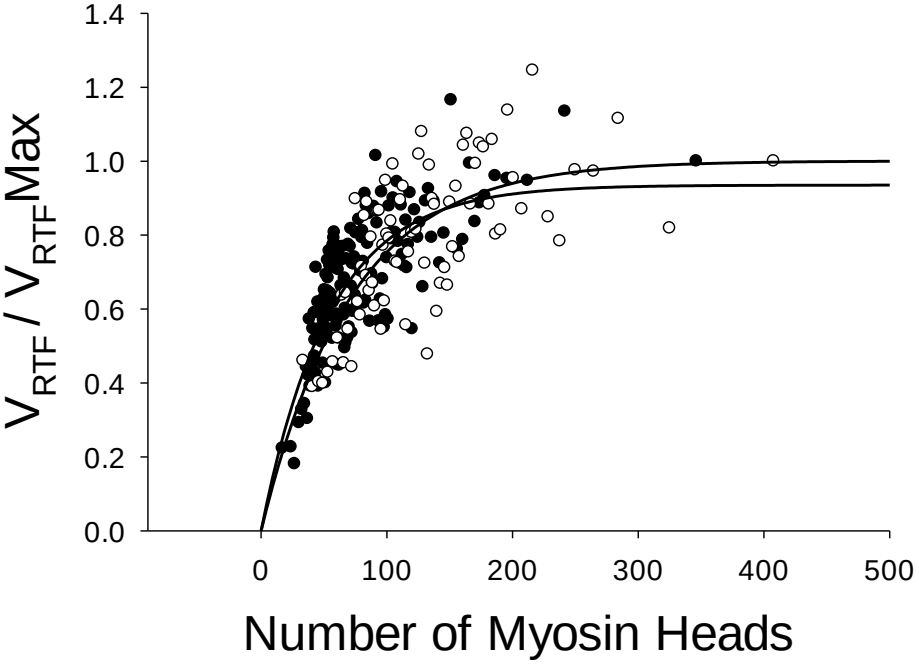

Figure 4.15. Same data as Figure 4.9, but shown here normalized to each Tn variant's peak velocity. This better shows how similar the duty cycle is between each condition.

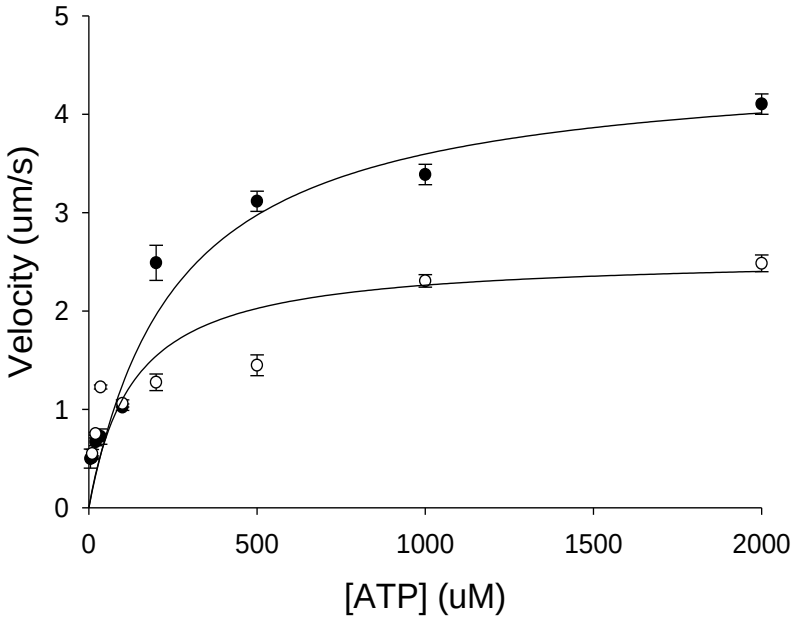

Figure 4.16. Velocity of each Tn variant as a function of ATP. By measuring velocity as a function of ATP, we can calculate the ADP release rate (table 4.3)

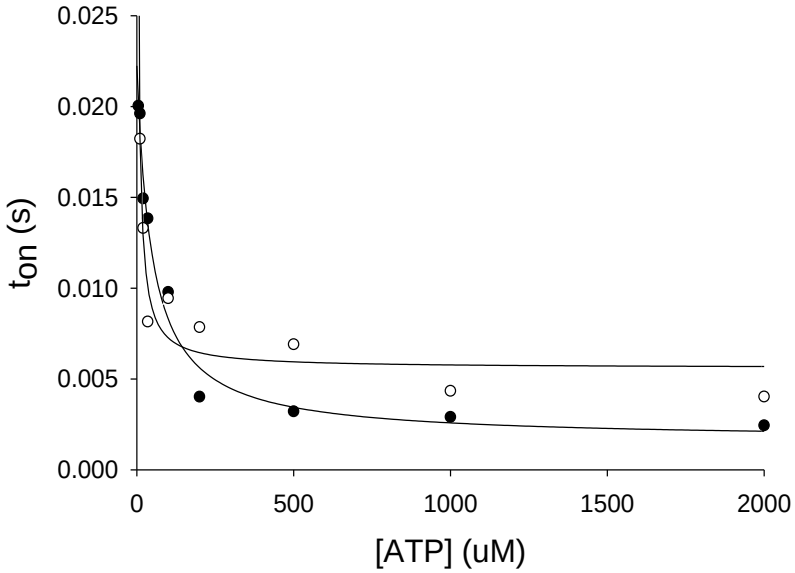

Figure 4.17. Using the same data in figure 4.11, we can calculate time on by measuring velocity and by assuming that myosin displaces actin 10 nm with each powerstroke.

REFERENCES

1. **Aboelkassem Y, Bonilla JA, McCabe KJ and Campbell SG.** Contributions of Ca2+-Independent Thin Filament Activation to Cardiac Muscle Function. *Biophys.J.* 109: 10: 2101-2112, 2015.

2. **Allen DG, Lamb GD and Westerblad H.** Skeletal muscle fatigue: cellular mechanisms. *Physiol.Rev.* 88: 1: 287-332, 2008.

3. **Allen DG, Lee JA and Westerblad H.** Intracellular calcium and tension during fatigue in isolated single muscle fibres from Xenopus laevis. *J.Physiol.* 415: 433-458, 1989.

4. **Babu A, Scordilis SP, Sonnenblick EH and Gulati J.** The control of myocardial contraction with skeletal fast muscle troponin C. *J.Biol.Chem.* 262: 12: 5815-5822, 1987.

5. **Baker JE, Brosseau C, Joel PB and Warshaw DM.** The biochemical kinetics underlying actin movement generated by one and many skeletal muscle myosin molecules. *Biophys.J.* 82: 4: 2134-2147, 2002.

6. **Ball KL, Johnson MD and Solaro RJ.** Isoform specific interactions of troponin I and troponin C determine pH sensitivity of myofibrillar Ca2+ activation. *Biochemistry* 33: 28: 8464-8471, 1994.

7. **Blanchard EM, Pan BS and Solaro RJ.** The effect of acidic pH on the ATPase activity and troponin Ca2+ binding of rabbit skeletal myofilaments. *J.Biol.Chem.* 259: 5: 3181-3186, 1984.

8. **Blanchard EM and Solaro RJ.** Inhibition of the activation and troponin calcium binding of dog cardiac myofibrils by acidic pH. *Circ.Res.* 55: 3: 382-391, 1984.

9. **Brandt PW, Diamond MS, Rutchik JS and Schachat FH.** Co-operative interactions between troponin-tropomyosin units extend the length of the thin filament in skeletal muscle. *J.Mol.Biol.* 195: 4: 885-896, 1987.

10. **Brandt PW, Diamond MS and Schachat FH.** The thin filament of vertebrate skeletal muscle co-operatively activates as a unit. *J.Mol.Biol.* 180: 2: 379-384, 1984.

11. **Bremel RD and Weber A.** Cooperation within actin filament in vertebrate skeletal muscle. *Nat.New Biol.* 238: 82: 97-101, 1972.

12. **Brunet NM, Chase PB, Mihajlovic G and Schoffstall B.** Ca(2+)-regulatory function of the inhibitory peptide region of cardiac troponin I is aided by the C-terminus of cardiac troponin T: Effects of familial hypertrophic cardiomyopathy mutations cTnI R145G and cTnT R278C, alone and in combination, on filament sliding. *Arch.Biochem.Biophys.* 552-553: 11-20, 2014.

13. **Cady EB, Jones DA, Lynn J and Newham DJ.** Changes in force and intracellular metabolites during fatigue of human skeletal muscle. *J.Physiol.* 418: 311-325, 1989.

14. **Campbell SG, Lionetti FV, Campbell KS and McCulloch AD.** Coupling of adjacent tropomyosins enhances cross-bridge-mediated cooperative activation in a markov model of the cardiac thin filament. *Biophys.J.* 98: 10: 2254-2264, 2010.

15. **Capitanio M, Canepari M, Maffei M, Beneventi D, Monico C, Vanzi F, Bottinelli R and Pavone FS.** Ultrafast force-clamp spectroscopy of single molecules reveals load dependence of myosin working stroke. *Nat.Methods* 9: 10: 1013-1019, 2012.

16. **Chalovich JM and Eisenberg E.** Inhibition of actomyosin ATPase activity by troponin-tropomyosin without blocking the binding of myosin to actin. *J.Biol.Chem.* 257: 5: 2432-2437, 1982.

17. **Clemmens EW and Regnier M.** Skeletal regulatory proteins enhance thin filament sliding speed and force by skeletal HMM. *J.Muscle Res.Cell.Motil.* 25: 7: 515-525, 2004.

18. **Cooke R and Pate E.** The effects of ADP and phosphate on the contraction of muscle fibers. *Biophys.J.* 48: 5: 789-798, 1985.

19. **Craig R and Lehman W.** Crossbridge and tropomyosin positions observed in native, interacting thick and thin filaments. *J.Mol.Biol.* 311: 5: 1027-1036, 2001.

20. **Dantzig JA, Goldman YE, Millar NC, Lacktis J and Homsher E.** Reversal of the cross-bridge force-generating transition by photogeneration of phosphate in rabbit psoas muscle fibres. *J.Physiol.* 451: 247-278, 1992.

21. **Dantzig JA, Hibberd MG, Trentham DR and Goldman YE.** Cross-bridge kinetics in the presence of MgADP investigated by photolysis of caged ATP in rabbit psoas muscle fibres. *J.Physiol.* 432: 639-680, 1991.

22. **Dargis R, Pearlstone JR, Barrette-Ng I, Edwards H and Smillie LB.** Single mutation (A162H) in human cardiac troponin I corrects acid pH sensitivity of Ca2+-regulated actomyosin S1 ATPase. *J.Biol.Chem.* 277: 38: 34662-34665, 2002.

23. **Dawson MJ, Gadian DG and Wilkie DR.** Muscular fatigue investigated by phosphorus nuclear magnetic resonance. *Nature* 274: 5674: 861-866, 1978.

24. **Day SM, Westfall MV, Fomicheva EV, Hoyer K, Yasuda S, La Cross NC, D'Alecy LG, Ingwall JS and Metzger JM.** Histidine button engineered into cardiac troponin I protects the ischemic and failing heart. *Nat.Med.* 12: 2: 181-189, 2006.

25. **Debold EP, Beck SE and Warshaw DM.** Effect of low pH on single skeletal muscle myosin mechanics and kinetics. *Am.J.Physiol.Cell.Physiol.* 295: 1: C173-9, 2008.

26. **Debold EP, Longyear TJ and Turner MA.** The effects of phosphate and acidosis on regulated thin filament velocity in an in vitro motility assay. *J.Appl.Physiol.* 2012.

27. **Debold EP, Patlak JB and Warshaw DM.** Slip sliding away: load-dependence of velocity generated by skeletal muscle myosin molecules in the laser trap. *Biophys.J.* 89: 5: L34-6, 2005.

28. **Debold EP, Walcott S, Woodward M and Turner MA.** Direct observation of phosphate inhibiting the force-generating capacity of a miniensemble of Myosin molecules. *Biophys.J.* 105: 10: 2374-2384, 2013.

29. **Desai RA, Geeves MA and Kad NM.** Using Fluorescent Myosin to Directly Visualize Cooperative Activation of Thin Filaments. *J.Biol.Chem.* 2014.

30. **Ding XL, Akella AB, Sonnenblick EH, Rao VG and Gulati J.** Molecular basis of depression of Ca2+ sensitivity of tension by acid pH in cardiac muscles of the mouse and the rat. *J.Card.Fail.* 2: 4: 319-326, 1996.

31. **Dunn AR and Spudich JA.** Dynamics of the unbound head during myosin V processive translocation. *Nat.Struct.Mol.Biol.* 14: 3: 246-248, 2007.

32. **Edwards RHT.** Biochemical Basis of Fatigue in Exercise Performance: Catastrophe Theory of Muscular Fatigue. In: Biochemistry of Exercise. *Human Kinetics* 3, 1983.

33. **Eisenberg E and Hill TL.** Muscle contraction and free energy transduction in biological systems. *Science* 227: 4690: 999-1006, 1985.

34. **Elliott K, Watkins H and Redwood CS.** Altered regulatory properties of human cardiac troponin I mutants that cause hypertrophic cardiomyopathy. *J.Biol.Chem.* 275: 29: 22069-22074, 2000.

35. **el-Saleh SC and Solaro RJ.** Troponin I enhances acidic pH-induced depression of Ca2+ binding to the regulatory sites in skeletal troponin C. *J.Biol.Chem.* 263: 7: 3274-3278, 1988.

36. **Farah CS, Miyamoto CA, Ramos CH, da Silva AC, Quaggio RB, Fujimori K, Smillie LB and Reinach FC.** Structural and regulatory functions of the NH2- and COOH-terminal regions of skeletal muscle troponin I. *J.Biol.Chem.* 269: 7: 5230-5240, 1994.

37. **Finer JT, Simmons RM and Spudich JA.** Single myosin molecule mechanics: piconewton forces and nanometre steps. *Nature* 368: 6467: 113-119, 1994.

38. **Fitts RH.** Cellular mechanisms of muscle fatigue. *Physiol.Rev.* 74: 1: 49-94, 1994.

39. **Fuchs F.** The binding of calcium to glycerinated muscle fibers in rigor. The effect of filament overlap. *Biochim.Biophys.Acta* 491: 2: 523-531, 1977.

40. **Fukuda N, Fujita H, Fujita T and Ishiwata S.** Regulatory roles of MgADP and calcium in tension development of skinned cardiac muscle. *J.Muscle Res.Cell.Motil.* 19: 8: 909-921, 1998.

41. **Fusi L, Brunello E, Sevrieva IR, Sun YB and Irving M.** Structural dynamics of troponin during activation of skeletal muscle. *Proc.Natl.Acad.Sci.U.S.A.* 111: 12: 4626-4631, 2014.

42. **Geeves M, Griffiths H, Mijailovich S and Smith D.** Cooperative [Ca(2)+]-dependent regulation of the rate of myosin binding to actin: solution data and the tropomyosin chain model. *Biophys.J.* 100: 11: 2679-2687, 2011.

43. **Georgiadou P and Adamopoulos S.** Skeletal muscle abnormalities in chronic heart failure. *Curr.Heart Fail.Rep.* 9: 2: 128-132, 2012.

44. **Gordon AM, Homsher E and Regnier M.** Regulation of contraction in striated muscle. *Physiol.Rev.* 80: 2: 853-924, 2000.

45. **Gordon AM, Regnier M and Homsher E.** Skeletal and cardiac muscle contractile activation: tropomyosin "rocks and rolls". *News Physiol.Sci.* 16: 49-55, 2001.

46. **Grabarek Z, Grabarek J, Leavis PC and Gergely J.** Cooperative binding to the Ca2+-specific sites of troponin C in regulated actin and actomyosin. *J.Biol.Chem.* 258: 23: 14098-14102, 1983.

47. **Greenberg MJ, Shuman H and Ostap EM.** Inherent force-dependent properties of beta-cardiac myosin contribute to the force-velocity relationship of cardiac muscle. *Biophys.J.* 107: 12: L41-4, 2014.

48. **Greene LE and Eisenberg E.** Cooperative binding of myosin subfragment-1 to the actin-troponin-tropomyosin complex. *Proc.Natl.Acad.Sci.U.S.A.* 77: 5: 2616-2620, 1980.

49. **Greene LE, Williams DL,Jr and Eisenberg E.** Regulation of actomyosin ATPase activity by troponin-tropomyosin: effect of the binding of the myosin subfragment 1 (S-1).ATP complex. *Proc.Natl.Acad.Sci.U.S.A.* 84: 10: 3102-3106, 1987.

50. **Guth K and Potter JD.** Effect of rigor and cycling cross-bridges on the structure of troponin C and on the Ca2+ affinity of the Ca2+-specific regulatory sites in skinned rabbit psoas fibers. *J.Biol.Chem.* 262: 28: 13627-13635, 1987.

51. **Harris DE and Warshaw DM.** Smooth and skeletal muscle myosin both exhibit low duty cycles at zero load in vitro. *J.Biol.Chem.* 268: 20: 14764-14768, 1993.

52. **Haselgrove JC.** The Mechanism of Muscle Contraction. *Cold Spring Harbor Symposia* XXXVII: p. 341, 1973.

53. **Heeley DH, Belknap B and White HD.** Mechanism of regulation of phosphate dissociation from actomyosin-ADP-Pi by thin filament proteins. *Proc.Natl.Acad.Sci.U.S.A.* 99: 26: 16731-16736, 2002.

54. **Herzberg O and James MN.** Structure of the calcium regulatory muscle protein troponin-C at 2.8 A resolution. *Nature* 313: 6004: 653-659, 1985.

55. **Hill AV.** The Heat of Shortening and the Dynamic Constants of Muscle. 126: 843: 136-195, 1938.

56. **Hoar PE, Mahoney CW and Kerrick WG.** MgADP- increases maximum tension and Ca2+ sensitivity in skinned rabbit soleus fibers. *Pflugers Arch.* 410: 1-2: 30-36, 1987.

57. **Homsher E, Kim B, Bobkova A and Tobacman LS.** Calcium regulation of thin filament movement in an in vitro motility assay. *Biophys.J.* 70: 4: 1881-1892, 1996.

58. **Huxley AF.** Muscle structure and theories of contraction. *Prog.Biophys.Biophys.Chem.* 7: 255-318, 1957.

59. **Huxley HE.** Sliding filaments and molecular motile systems. *J.Biol.Chem.* 265: 15: 8347-8350, 1990.

60. **James J, Zhang Y, Osinska H, Sanbe A, Klevitsky R, Hewett TE and Robbins J.** Transgenic modeling of a cardiac troponin I mutation linked to familial hypertrophic cardiomyopathy. *Circ.Res.* 87: 9: 805-811, 2000.

61. **Johnson D, Mathur MC, Kobayashi T and Chalovich JM.** The Cardiomyopathy Mutation, R146G Troponin I, Stabilizes the Intermediate "C" State of Regulated Actin under High- and Low-Free Ca(2+) Conditions. *Biochemistry* 55: 32: 4533-4540, 2016.

62. **Kad NM, Kim S, Warshaw DM, VanBuren P and Baker JE.** Single-myosin crossbridge interactions with actin filaments regulated by troponin-tropomyosin. *Proc.Natl.Acad.Sci.U.S.A.* 102: 47: 16990-16995, 2005.

63. **Karatzaferi C, Franks-Skiba K and Cooke R.** Inhibition of shortening velocity of skinned skeletal muscle fibers in conditions that mimic fatigue. *Am.J.Physiol.Regul.Integr.Comp.Physiol.* 294: 3: R948-55, 2008.

64. **Kent-Braun JA.** Central and peripheral contributions to muscle fatigue in humans during sustained maximal effort. *Eur.J.Appl.Physiol.Occup.Physiol.* 80: 1: 57-63, 1999.

65. **Kimura A, Harada H, Park JE, Nishi H, Satoh M, Takahashi M, Hiroi S, Sasaoka T, Ohbuchi N, Nakamura T, Koyanagi T, Hwang TH, Choo JA, Chung KS, Hasegawa A, Nagai R, Okazaki O, Nakamura H, Matsuzaki M, Sakamoto T, Toshima H, Koga Y, Imaizumi T and Sasazuki T.** Mutations in the cardiac troponin I gene associated with hypertrophic cardiomyopathy. *Nat.Genet.* 16: 4: 379-382, 1997.

66. **Knight AE, Veigel C, Chambers C and Molloy JE.** Analysis of single-molecule mechanical recordings: application to acto-myosin interactions. *Prog.Biophys.Mol.Biol.* 77: 1: 45-72, 2001.

67. **Knuth ST, Dave H, Peters JR and Fitts RH.** Low cell pH depresses peak power in rat skeletal muscle fibres at both 30 degrees C and 15 degrees C: implications for muscle fatigue. *J.Physiol.* 575: Pt 3: 887-899, 2006.

68. **Kovacs M, Toth J, Hetenyi C, Malnasi-Csizmadia A and Sellers JR.** Mechanism of blebbistatin inhibition of myosin II. *J.Biol.Chem.* 279: 34: 35557-35563, 2004.

69. **Kruger M, Zittrich S, Redwood C, Blaudeck N, James J, Robbins J, Pfitzer G and Stehle R.** Effects of the mutation R145G in human cardiac troponin I on the kinetics of the contraction-relaxation cycle in isolated cardiac myofibrils. *J.Physiol.* 564: Pt 2: 347-357, 2005.

70. **Lang R, Gomes AV, Zhao J, Housmans PR, Miller T and Potter JD.** Functional analysis of a troponin I (R145G) mutation associated with familial hypertrophic cardiomyopathy. *J.Biol.Chem.* 277: 14: 11670-11678, 2002.

71. **Lee JA, Westerblad H and Allen DG.** Changes in tetanic and resting [Ca2+]i during fatigue and recovery of single muscle fibres from Xenopus laevis. *J.Physiol.* 433: 307-326, 1991.

72. **Lehrer SS and Morris EP.** Dual effects of tropomyosin and troponin-tropomyosin on actomyosin subfragment 1 ATPase. *J.Biol.Chem.* 257: 14: 8073-8080, 1982.

73. **Leonard TR and Herzog W.** Regulation of muscle force in the absence of actin-myosin-based cross-bridge interaction. *Am.J.Physiol.Cell.Physiol.* 299: 1: C14-20, 2010.

74. **Li XE, Holmes KC, Lehman W, Jung H and Fischer S.** The shape and flexibility of tropomyosin coiled coils: implications for actin filament assembly and regulation. *J.Mol.Biol.* 395: 2: 327-339, 2010.

75. **Lindhout DA, Li MX, Schieve D and Sykes BD.** Effects of T142 phosphorylation and mutation R145G on the interaction of the inhibitory region of human cardiac troponin I with the C-domain of human cardiac troponin C. *Biochemistry* 41: 23: 7267-7274, 2002.

76. **Longyear TJ, Turner MA, Davis JP, Lopez J, Biesiadecki B and Debold EP.** Ca++-sensitizing mutations in troponin, P(i), and 2-deoxyATP alter the depressive effect of acidosis on regulated thin-filament velocity. *J.Appl.Physiol.(1985)* 116: 9: 1165-1174, 2014.

77. **Loong CK, Zhou HX and Chase PB.** Persistence length of human cardiac alpha-tropomyosin measured by single molecule direct probe microscopy. *PLoS One* 7: 6: e39676, 2012.

78. **Margossian SS and Lowey S.** Preparation of myosin and its subfragments from rabbit skeletal muscle. *Methods Enzymol.* 85 Pt B: 55-71, 1982.

79. **Marsiglia JD and Pereira AC.** Hypertrophic cardiomyopathy: how do mutations lead to disease? *Arq.Bras.Cardiol.* 102: 3: 295-304, 2014.

80. **Maytum R, Lehrer SS and Geeves MA.** Cooperativity and switching within the three-state model of muscle regulation. *Biochemistry* 38: 3: 1102-1110, 1999.

81. **McKillop DF and Geeves MA.** Regulation of the interaction between actin and myosin subfragment 1: evidence for three states of the thin filament. *Biophys.J.* 65: 2: 693-701, 1993.

82. **Metzger JM and Moss RL.** Effects of tension and stiffness due to reduced pH in mammalian fast- and slow-twitch skinned skeletal muscle fibres. *J.Physiol.* 428: 737-750, 1990.

83. **Metzger JM and Moss RL.** pH modulation of the kinetics of a Ca2(+)-sensitive cross-bridge state transition in mammalian single skeletal muscle fibres. *J.Physiol.* 428: 751-764, 1990.

84. **Mijailovich SM, Kayser-Herold O, Li X, Griffiths H and Geeves MA.** Cooperative regulation of myosin-S1 binding to actin filaments by a continuous flexible Tm-Tn chain. *Eur.Biophys.J.* 41: 12: 1015-1032, 2012.

85. **Millar NC and Homsher E.** The effect of phosphate and calcium on force generation in glycerinated rabbit skeletal muscle fibers. A steady-state and transient kinetic study. *J.Biol.Chem.* 265: 33: 20234-20240, 1990.

86. **Morimoto S, Harada K and Ohtsuki I.** Roles of troponin isoforms in pH dependence of contraction in rabbit fast and slow skeletal and cardiac muscles. *J.Biochem.* 126: 1: 121-129, 1999.

87. **Moss RL, Allen JD and Greaser ML.** Effects of partial extraction of troponin complex upon the tension-pCa relation in rabbit skeletal muscle. Further evidence that tension development involves cooperative effects within the thin filament. *J.Gen.Physiol.* 87: 5: 761-774, 1986.

88. **Nelson CR and Fitts RH.** Effects of low cell pH and elevated inorganic phosphate on the pCa-force relationship in single muscle fibers at near-physiological temperatures. *Am.J.Physiol.Cell.Physiol.* 306: 7: C670-8, 2014.

89. **Nishizaka T, Miyata H, Yoshikawa H, Ishiwata S and Kinosita K,Jr.** Unbinding force of a single motor molecule of muscle measured using optical tweezers. *Nature* 377: 6546: 251-254, 1995.

90. **Nishizaka T, Seo R, Tadakuma H, Kinosita K,Jr and Ishiwata S.** Characterization of single actomyosin rigor bonds: load dependence of lifetime and mechanical properties. *Biophys.J.* 79: 2: 962-974, 2000.

91. **Nyitrai M, Rossi R, Adamek N, Pellegrino MA, Bottinelli R and Geeves MA.** What limits the velocity of fast-skeletal muscle contraction in mammals? *J.Mol.Biol.* 355: 3: 432-442, 2006.

92. **Pardee JD and Spudich JA.** Purification of muscle actin. *Methods Enzymol.* 85 Pt B: 164-181, 1982.

93. **Parsons B, Szczesna D, Zhao J, Van Slooten G, Kerrick WG, Putkey JA and Potter JD.** The effect of pH on the Ca2+ affinity of the Ca2+ regulatory sites of skeletal and cardiac troponin C in skinned muscle fibres. *J.Muscle Res.Cell.Motil.* 18: 5: 599-609, 1997.

94. **Pastra-Landis SC, Huiatt T and Lowey S.** Assembly and kinetic properties of myosin light chain isozymes from fast skeletal muscle. *J.Mol.Biol.* 170: 2: 403-422, 1983.

95. **Pate E, Bhimani M, Franks-Skiba K and Cooke R.** Reduced effect of pH on skinned rabbit psoas muscle mechanics at high temperatures: implications for fatigue. *J.Physiol.* 486 (Pt 3): Pt 3: 689-694, 1995.

96. **Pedersen TH, Nielsen OB, Lamb GD and Stephenson DG.** Intracellular acidosis enhances the excitability of working muscle. *Science* 305: 5687: 1144-1147, 2004.

97. **Phillips GN,Jr and Chacko S.** Mechanical properties of tropomyosin and implications for muscle regulation. *Biopolymers* 38: 1: 89-95, 1996.

98. **Phillips GN,Jr, Fillers JP and Cohen C.** Tropomyosin crystal structure and muscle regulation. *J.Mol.Biol.* 192: 1: 111-131, 1986.

99. **Pinsky JL, Jette AM, Branch LG, Kannel WB and Feinleib M.** The Framingham Disability Study: relationship of various coronary heart disease manifestations to disability in older persons living in the community. *Am.J.Public Health* 80: 11: 1363-1367, 1990.

100. **Potma EJ, van Graas IA and Stienen GJ.** Effects of pH on myofibrillar ATPase activity in fast and slow skeletal muscle fibers of the rabbit. *Biophys.J.* 67: 6: 2404-2410, 1994.

101. **Regnier M and Homsher E.** The effect of ATP analogs on posthydrolytic and force development steps in skinned skeletal muscle fibers. *Biophys.J.* 74: 6: 3059-3071, 1998.

102. **Regnier M, Lee DM and Homsher E.** ATP analogs and muscle contraction: mechanics and kinetics of nucleoside triphosphate binding and hydrolysis. *Biophys.J.* 74: 6: 3044-3058, 1998.

103. **Regnier M, Rivera AJ, Wang CK, Bates MA, Chase PB and Gordon AM.** Thin filament near-neighbour regulatory unit interactions affect rabbit skeletal muscle steady-state force-Ca(2+) relations. *J.Physiol.* 540: Pt 2: 485-497, 2002.

104. **Reuben JP, Brandt PW, Berman M and Grundfest H.** Regulation of tension in the skinned crayfish muscle fiber. I. Contraction and relaxation in the absence of Ca (pCa is greater than 9). *J.Gen.Physiol.* 57: 4: 385-407, 1971.

105. **Seow CY and Ford LE.** High ionic strength and low pH detain activated skinned rabbit skeletal muscle crossbridges in a low force state. *J.Gen.Physiol.* 101: 4: 487-511, 1993.

106. **Sleep JA and Hutton RL.** Exchange between inorganic phosphate and adenosine 5'-triphosphate in the medium by actomyosin subfragment 1. *Biochemistry* 19: 7: 1276-1283, 1980.

107. **Sleep JA and Hutton RL.** Actin mediated release of ATP from a myosin-ATP complex. *Biochemistry* 17: 25: 5423-5430, 1978.

108. **Sousa DR, Stagg SM and Stroupe ME.** Cryo-EM structures of the actin:tropomyosin filament reveal the mechanism for the transition from C- to M-state. *J.Mol.Biol.* 425: 22: 4544-4555, 2013.

109. **Stienen GJ, Papp Z and Zaremba R.** Influence of inorganic phosphate and pH on sarcoplasmic reticular ATPase in skinned muscle fibres of Xenopus laevis. *J.Physiol.* 518 (Pt 3): Pt 3: 735-744, 1999.

110. **Sung J, Nag S, Mortensen KI, Vestergaard CL, Sutton S, Ruppel K, Flyvbjerg H and Spudich JA.** Harmonic force spectroscopy measures load-dependent kinetics of individual human beta-cardiac myosin molecules. *Nat.Commun.* 6: 7931, 2015.

111. **Swartz DR and Moss RL.** Influence of a strong-binding myosin analogue on calcium-sensitive mechanical properties of skinned skeletal muscle fibers. *J.Biol.Chem.* 267: 28: 20497-20506, 1992.

112. **Swartz DR, Moss RL and Greaser ML.** Calcium alone does not fully activate the thin filament for S1 binding to rigor myofibrils. *Biophys.J.* 71: 4: 1891-1904, 1996.

113. **Syska H, Wilkinson JM, Grand RJ and Perry SV.** The relationship between biological activity and primary structure of troponin I from white skeletal muscle of the rabbit. *Biochem.J.* 153: 2: 375-387, 1976.

114. **Takahashi-Yanaga F, Morimoto S, Harada K, Minakami R, Shiraishi F, Ohta M, Lu QW, Sasaguri T and Ohtsuki I.** Functional consequences of the mutations in human cardiac troponin I gene found in familial hypertrophic cardiomyopathy. *J.Mol.Cell.Cardiol.* 33: 12: 2095-2107, 2001.

115. **Talbot JA and Hodges RS.** Synthetic studies on the inhibitory region of rabbit skeletal troponin I. Relationship of amino acid sequence to biological activity. *J.Biol.Chem.* 256: 6: 2798-2802, 1981.

116. **Tanner BC, Daniel TL and Regnier M.** Sarcomere lattice geometry influences cooperative myosin binding in muscle. *PLoS Comput.Biol.* 3: 7: e115, 2007.

117. **Tobacman LS and Butters CA.** A new model of cooperative myosin-thin filament binding. *J.Biol.Chem.* 275: 36: 27587-27593, 2000.

118. **Trybus KM and Taylor EW.** Kinetic studies of the cooperative binding of subfragment 1 to regulated actin. *Proc.Natl.Acad.Sci.U.S.A.* 77: 12: 7209-7213, 1980.

119. **Tyska MJ, Dupuis DE, Guilford WH, Patlak JB, Waller GS, Trybus KM, Warshaw DM and Lowey S.** Two heads of myosin are better than one for generating force and motion. *Proc.Natl.Acad.Sci.U.S.A.* 96: 8: 4402-4407, 1999.

120. **Uyeda TQ, Kron SJ and Spudich JA.** Myosin step size. Estimation from slow sliding movement of actin over low densities of heavy meromyosin. *J.Mol.Biol.* 214: 3: 699-710, 1990.

121. **Veigel C, Molloy JE, Schmitz S and Kendrick-Jones J.** Load-dependent kinetics of force production by smooth muscle myosin measured with optical tweezers. *Nat.Cell Biol.* 5: 11: 980-986, 2003.

122. **Vibert P, Craig R and Lehman W.** Steric-model for activation of muscle thin filaments. *J.Mol.Biol.* 266: 1: 8-14, 1997.

123. **Vinogradova MV, Stone DB, Malanina GG, Karatzaferi C, Cooke R, Mendelson RA and Fletterick RJ.** Ca(2+)-regulated structural changes in troponin. *Proc.Natl.Acad.Sci.U.S.A.* 102: 14: 5038-5043, 2005.

124. **von der Ecken J, Heissler SM, Pathan-Chhatbar S, Manstein DJ and Raunser S.** Cryo-EM structure of a human cytoplasmic actomyosin complex at near-atomic resolution. *Nature* 534: 7609: 724-728, 2016.

125. **von der Ecken J, Muller M, Lehman W, Manstein DJ, Penczek PA and Raunser S.** Structure of the F-actin-tropomyosin complex. *Nature* 519: 7541: 114-117, 2015.

126. **Walcott S.** Muscle activation described with a differential equation model for large ensembles of locally coupled molecular motors. *Phys.Rev.E.Stat.Nonlin Soft Matter Phys.* 90: 4: 042717, 2014.

127. **Walcott S and Kad NM.** Direct Measurements of Local Coupling between Myosin Molecules Are Consistent with a Model of Muscle Activation. *PLoS Comput.Biol.* 11: 11: e1004599, 2015.

128. **Walcott S, Warshaw DM and Debold EP.** Mechanical Coupling between Myosin Molecules Causes Differences between Ensemble and Single-Molecule Measurements. *Biophys.J.* 103: 3: 501-510, 2012.

129. **Wen Y, Pinto JR, Gomes AV, Xu Y, Wang Y, Wang Y, Potter JD and Kerrick WG.** Functional consequences of the human cardiac troponin I hypertrophic cardiomyopathy mutation R145G in transgenic mice. *J.Biol.Chem.* 283: 29: 20484-20494, 2008.

130. **Westerblad H and Allen DG.** Changes of myoplasmic calcium concentration during fatigue in single mouse muscle fibers. *J.Gen.Physiol.* 98: 3: 615-635, 1991.

131. **Westfall MV, Albayya FP, Turner II and Metzger JM.** Chimera analysis of troponin I domains that influence Ca(2+)-activated myofilament tension in adult cardiac myocytes. *Circ.Res.* 86: 4: 470-477, 2000.

132. **Westfall MV, Borton AR, Albayya FP and Metzger JM.** Myofilament calcium sensitivity and cardiac disease: insights from troponin I isoforms and mutants. *Circ.Res.* 91: 6: 525-531, 2002.

133. **Westfall MV and Metzger JM.** Single amino acid substitutions define isoform-specific effects of troponin I on myofilament Ca2+ and pH sensitivity. *J.Mol.Cell.Cardiol.* 43: 2: 107-118, 2007.

134. **Wilson JR, McCully KK, Mancini DM, Boden B and Chance B.** Relationship of muscular fatigue to pH and diprotonated Pi in humans: a 31P-NMR study. *J.Appl.Physiol.* 64: 6: 2333-2339, 1988.

135. **Wolska BM, Vijayan K, Arteaga GM, Konhilas JP, Phillips RM, Kim R, Naya T, Leiden JM, Martin AF, de Tombe PP and Solaro RJ.** Expression of slow skeletal troponin I in adult transgenic mouse heart muscle reduces the force decline observed during acidic conditions. *J.Physiol.* 536: Pt 3: 863-870, 2001.

136. **Wu M, Roberts JW and Buckley M.** Three-dimensional fluorescent particle tracking at micron-scale using a single camera. *Exp in Fluids* 38: 461, 2005.

137. **Zhao Y and Kawai M.** Kinetic and thermodynamic studies of the cross-bridge cycle in rabbit psoas muscle fibers. *Biophys.J.* 67: 4: 1655-1668, 1994.

138. **Zhou Z, Rieck D, Li KL, Ouyang Y and Dong WJ.** Structural and kinetic effects of hypertrophic cardiomyopathy related mutations R146G/Q and R163W on the regulatory switching activity of rat cardiac troponin I. *Arch.Biochem.Biophys.* 535: 1: 56-67, 2013.